Genome scans on experimentally evolved populations reveal candidate regions for adaptation to plant resistance in the potato cyst nematode Globodera pallida.

Delphine Eoche-Bosy, Matthieu Gautier, Magali Esquibet, Fabrice Legeai, Anthony Bretaudeau, Olivier Bouchez, Sylvain Fournet, Eric Grenier, Josselin Montarry

Genome scans on experimentally evolved populations reveal candidate regions for adaptation to plant resistance in the potato cyst nematode *Globodera pallida*

D. EOCHE-BOSY[1], M. GAUTIER[2,3], M. ESQUIBET[1], F. LEGEAI[4,5], A. BRETAUDEAU[4,6], O. BOUCHEZ[7,8], S. FOURNET[1], E. GRENIER[1] and J. MONTARRY[1]

[1]IGEPP, INRA, Agrocampus Ouest, Université de Rennes 1, 35650, Le Rheu, France

[2]CBGP, INRA, IRD, CIRAD, Montpellier SupAgro, 34988, Montferrier-sur-Lez, France

[3]IBC, 34095, Montpellier, France

[4]IGEPP, BIPAA, INRA, Agrocampus Ouest, Université de Rennes 1, 35042, Rennes, France

[5]IRISA, GenScale, INRIA, 35042, Rennes, France

[6]IRISA, GenOuest COre Facility, INRIA, 35042, Rennes, France

[7]GeT-PlaGe, Genotoul, INRA, 31326, Castanet-Tolosan, France

[8]GenPhySE, Université de Toulouse, INRA, INPT, ENVT, 31326, Castanet-Tolosan, France

Keywords evolve and resequence; experimental evolution; Pool-Seq; population genomics; selection; virulence

Correspondence: Josselin Montarry, IGEPP, INRA, Agrocampus Ouest, Université de Rennes 1, 35650, Le Rheu, France; Fax: +33 2 23 48 51 50; E-mail: josselin.montarry@inra.fr

Running title: Molecular signatures of adaptation to resistance

Abstract

Improving resistance durability involves to be able to predict the adaptation speed of pathogen populations. Identifying the genetic bases of pathogen adaptation to plant resistances is a useful step to better understand and anticipate this phenomenon. *Globodera pallida* is a major pest of potato crop for which a resistance QTL, $GpaV_{vrn}$, has been identified in *Solanum vernei*. However, its durability is threatened as *G. pallida* populations are able to adapt to the resistance in few generations. The aim of the present study was to investigate the genomic regions involved in the resistance breakdown by coupling experimental evolution and high density genome scan. We performed a whole genome resequencing of pools of individuals (Pool-Seq) belonging to *G. pallida* lineages derived from two independent populations having experimentally evolved on susceptible and resistant potato cultivars. About 1.6 million SNPs were used to perform the genome scan using a recent model testing for adaptive differentiation and association to population-specific covariables. We identified 275 outliers and 31 of them, which also showed a significant reduction of diversity in adapted lineages, were investigated for their genic environment. Some candidate genomic regions contained genes putatively encoding effectors and were enriched in SPRYSECs, known in cyst nematodes to be involved in pathogenicity and in (a)virulence. Validated candidate SNPs will provide a useful molecular tool to follow frequencies of virulence alleles in natural *G. pallida* populations and define efficient strategies of use of potato resistances maximizing their durability.

Introduction

Because of the threat caused by crop pathogens to global food security, control methods to limit yield losses and maintain sustainable productions are needed. If pesticides have been successfully employed for years, the current societal and political demand for a reduction of their use is strong. In most cases, resistant cultivars are now the chosen alternative, as they can be highly effective, organism-specific, economically and environmentally sustainable. However, this control method can be limited by evolutionary capacities of targeted pathogens, which can adapt to plant resistances (McDonald & Linde 2002). Resistance breakdowns have been documented in a wide range of crop pathogens, such as virus, bacteria, nematodes, fungi or oomycetes (e.g., Castagnone-Sereno 2002; McDonald & Linde 2002; Janzac *et al.* 2009), whereas the development of resistant cultivars is a long process, in the order of decades, *i.e.* usually longer than the time needed for pathogen populations to overcome resistances. Consequently, the design of strategies allowing an increase in resistance durability has been a major goal in plant pathology research over the last 50 years, especially as resistance genes or QTLs remain a scarce resource. To be efficient, such strategies have to integrate knowledge on the adaptation of pathogen populations to the selective pressure imposed by the resistant plant. Consequently, a significant step towards a better management of resistance durability could be taken by identifying the genetic determinants of adaptation to plant resistances, which would represent direct predictors allowing to link dynamics and genetics of resistance breakdown.

Plant-parasitic nematodes are major agricultural pathogens causing severe damages in crops worldwide (Nicol *et al.* 2011), but sources of resistance against them remain scarce. Several studies have been conducted to optimize the management of these resistances (Djian-Caporalino *et al.* 2014; Barbary *et al.* 2015). Cyst nematodes are among the most

economically damaging plant-parasitic nematodes. Over the last few years, increased knowledge about characteristics of cyst nematode populations allowed to better predict the global evolutionary potential of these populations. In particular it was showed that cyst nematode populations represent a real threat to the durability of plant resistances due to an important passive dispersion (Picard *et al.* 2004; Plantard & Porte 2004; Alenda *et al.* 2014) and favored expression of recessives virulence genes due to inbreeding (Montarry *et al.* 2015). The adaptation speed of nematode populations would also be modulated by the number and the nature of genetic mutations required to overcome the plant resistance, and by the presence and, if any, the frequency, of virulent individuals in fields.

The cyst nematode *Globodera pallida* (Stone) is a major pest of potato crop (Oerke *et al.* 1994; van Riel & Mulder 1998) and *Solanum vernei*, a wild potato species, is an interesting source of resistance against *G. pallida* as it is highly effective. The resistance, which leads to the development of most nematodes into adult males, is explained at 61% by the major QTL $GpaV_{vrn}$ mapped on the potato chromosome V (Rouppe van der Voort *et al.* 2000). This source of resistance is to date the only one exploited in commercial potato cultivars at the European level. The resistant cultivar Iledher, carrying $GpaV_{vrn}$, has been registered in 2009 in the French catalogue as the first cultivar showing a high level of resistance to *G. pallida*. However, Fournet *et al.* (2013) highlighted that *G. pallida* populations were able to completely overcome the resistance of Iledher in only few generations in experimental evolution. Identifying the determinants of virulence thus appears to be crucial to better anticipate the speed of adaptation of *G. pallida* populations.

In organisms with relatively small genomes, such as RNA viruses with 10-15 kb genomes, it is possible since several years to sequence the entire genome and to directly compare sequences of virulent and avirulent strains in order to find the mutation responsible

for resistance adaptation (Meshi *et al.* 1988; Díaz *et al.* 2004; Ayme *et al.* 2006; Mardis 2008; Janzac *et al.* 2010). However, this approach cannot be considered in eukaryotic organisms whose genomes range from one to hundreds of thousands megabases. Genome scans represent an efficient alternative to target genomic regions involved in adaptation in such organisms, as they analyze genome-wide variations at the light of theoretical predictions about the effects of selection, in order to detect locus specific signatures of positive directional selection (Luikart *et al.* 2003; Storz 2005). Despite their strong potential to elucidate the genetic bases of adaptation, genome scans have never been used to identify the determinants of virulence in nematodes. However, Bekal *et al.* (2015) recently opened the way for population genomic approach in cyst nematodes. They performed a whole genome allelic imbalance analysis of SNP in *Heterodera glycines* inbred lines grown in the laboratory for over 30 generations on resistant and susceptible soybean plants. This study revealed two new candidate virulence genes: *HgBioB*, a gene encoded biotin synthase and *HgSLP-1*, a gene that appears to have entered *H. glycines* genome via horizontal gene transfer and which encode a protein containing a putative SNARE domain. Virulence is based on sequence polymorphisms for the first gene and on a reduced copy number for the second gene. In potato cyst nematodes, (a)virulence genes known to date were identified only through candidate gene approaches. In *Globodera rostochiensis*, the venom allergen Gr-VAP1 was identified as an avirulence gene product triggering a cell death response in tomato (*Lycopersicon esculentum*) plants containing the *Cf-2* and *Rcr3pim* resistant genes (Lozano-Torres *et al.* 2012, 2014). In *G. pallida*, only one avirulence gene, *Gp-RBP-1*, coding for a SPRYSEC which interacts with the GPA2 resistant protein in potato, has been described (Sacco *et al.* 2009). Virulence is due to a single amino-acid polymorphism, however this mutation is widely distributed in European populations (Carpentier *et al.* 2012) and therefore

potato carrying *Gpa2* resistance gene is of very limited interest for control of *G. pallida*. On the contrary, the resistant cultivar Iledher shows a high level of resistance to a wide range of European *G. pallida* populations.

The aim of the present study was to investigate the *G. pallida* genomic regions involved in the breakdown of the resistance of potato cultivar Iledher. By analyzing microsatellite data, Eoche-Bosy *et al.* (2016) already showed that a genome scan on the *G. pallida* lineages coming from the experimental evolution performed by Fournet *et al.* (2013) was feasible. Here, we took advantage of the same biological material to perform a high density genome scan using data from a whole genome resequencing of pools of individuals (Pool-Seq, Futschik & Schlötterer 2010; Zhu *et al.* 2012; Ferretti *et al.* 2013; Gautier *et al.* 2013; Schlötterer *et al.* 2014) and a recent model testing for adaptive differentiation and association to population-specific covariables (BayPass, Gautier 2015).

Materials and methods

Study system: Globodera pallida

Globodera pallida is a gonochoristic diploid organism with obligate sexual reproduction, which achieves one generation per year in European climatic conditions (Jones 1950). This obligate parasite enters the plant roots as second-stage juveniles (J2) and establishes a specialized feeding structure, the syncytium (Jones & Northcote 1972), which is a severe nutrient sink for the plant. In this species, sex is environmentally determined and depends on the size and efficiency of the syncytium (Sobczak & Golinowski 2011). Adult males leave the root to mate females, which can be fertilized by several males (Green *et al.* 1970; Triantaphyllou & Esbenshade 1990). After mating, the females continue to feed from the

140 syncytium and when eggs development is completed, they die and form a cyst, enclosing
141 hundreds of eggs, which can stay viable for several years in soils.

142 The genome of *G. pallida* has been recently sequenced (Gpal.v1.0, Cotton *et al.* 2014).
143 It is available as an assembly of 124.7 Mb in 6,873 scaffolds, with a N50 of 122 kb and a GC
144 content of 36.7% (Cotton *et al.* 2014). Combining transcriptomic data with manual curation, a
145 total of 16,419 genes were predicted. The genome of *G. rostochiensis* has also been recently
146 sequenced (nGr.v1.0, Eves-van den Akker *et al.* 2016) and could be a more accurate
147 representation of a *Globodera* genome, as suggested by its higher completeness and low level
148 of gene duplication. This genome is available as an assembly of 95.9 Mb in 4,377 scaffolds,
149 with a N50 of 88 kb and a GC content of 38.1%. Annotation of *G. rostochiensis* genome
150 could also be of better quality as a manual annotation phase followed the initial phase of
151 automated annotation, resulting in the prediction of 14,378 genes.

152

153 *Selection of virulent and avirulent* G. pallida *lineages*

154 This study relies on the biological material coming from the experimental evolution
155 performed by Fournet *et al.* (2013). Briefly, nematode lineages were established from cysts of
156 two French natural *G. pallida* populations, SM (near Saint-Malo, Brittany, north-western
157 France) and N (from the island of Noirmoutier, western France) coming from infested fields
158 (Fig. 1). The lineages used here were obtained by rearing both populations during eight
159 successive cycles (*i.e.* eight generations) on the susceptible potato cultivar Désirée (D) and on
160 the resistant cultivar Iledher (I). The present study was conducted with the eighth generation
161 of the four lineages: two lineages adapted to the resistance of Iledher (named hereafter SMI
162 and NI), and two lineages which remained unadapted (named hereafter SMD and ND).

163

Pool sequencing

As the amount of DNA in a single *G. pallida* individual is very low, pooling individuals from a same lineage was an efficient way to increase the amount of DNA while allowing the accurate estimation of population allele frequencies (e.g., Gautier *et al.* 2013). To accurately represent the genetic variability of each lineage, we chose to sample individuals from different cysts, rather than different individuals from a same cyst, to constitute the pools. We therefore sampled 300 cysts in each lineage, which was the maximum available, and crushed them individually in sterile water. Two J2 (siblings) were sampled from each cyst and attributed to two different pools, resulting in two pools of 300 individuals for each lineage, *i.e.* two biological replicates. Water in samples was then vacuum-evaporated in a heated Speed Vac Concentrator (MiVac, Genevac Ltd., Ipswich, UK). As the cuticle of the nematode could prevent the lysis of tissues by the proteinase K, samples were stored at -80°C during two hours and then rapidly heated at ambient temperature, just before DNA extraction. DNA was extracted directly from each pool using Qiagen DNeasy Blood and Tissue Kit (Qiagen, Hilden, Germany) following the manufacturer's instructions. A pooled DNA extraction has been favored over an individual DNA extraction following by a pooling of the DNA in equimolar proportions because this last strategy can lead to heterogeneity in the amount of each individual DNA due to measurement (poor estimations of individuals DNA concentration) or pipetting errors (Gautier *et al.* 2013). Extracted genomic DNA was quantified using a Qubit® 2.0 Fluorometer (Invitrogen, Carlsbad, CA, USA) and quality was estimated using a Nanodrop® ND-2000 Spectrophotometer (Thermo Fisher Scientific, Wilmington, DE, USA). The DNA samples conformed to the required purity criteria (A260/A230 and A260/A280 > 1.8) for gDNA library preparation for sequencing, but not to the required concentration criterion, as the amount of DNA obtained from a 300 individuals

pool was still very low (*i.e.* 17 ng of DNA per pool on average). Paired-end libraries were therefore constructed from the totality of DNA available in each pool (*i.e.* each biological replicate in each lineage) contained in 100 µL AE buffer (Qiagen), using the TruSeq Nano DNA Sample Preparation Kits (Illumina, San Diego, CA, USA), according to the manufacturer's instructions. Briefly, DNA was fragmented using a Covaris M220 ultrasonicator (Covaris, Woburn, MA, USA) and, after a purification step, end repaired. A bead-based size selection was performed, then DNA was A-tailed and ligated to indexed sequencing adapters (60 bp on each side), each biological replicate being identified by a different index. After a double-purification, libraries were enriched by eight PCR cycles, followed by a final purification. Library profiles were controlled using a DNA High Sensitivity chip on a BioAnalyzer 2100 (Agilent Technologies, Santa Clara, CA, USA), showing that the average size of the eight libraries was 513 bp (*i.e.* average insert size of 493 bp). Libraries were then quantified by qPCR on ABI7900HT (Applied Biosystems) in order to pool them in equimolar proportions. The final pool was again quantified by qPCR on ABI7900HT in order to load on each lane a volume corresponding to a DNA concentration of 8 pM. In order to sequence the eight libraries at an expected 150X coverage depth, four lanes were necessary. Sequencing was performed on an Illumina HiSeq™ 2500 platform (Illumina). Three lanes were sequenced with HiSeq v4 reagent kits (HiSeq PE Cluster Kit v4 and HiSeq SBS Kit v4, Illumina) providing 2x125 bp paired-end reads and the fourth lane was sequenced with TruSeq v3 reagents kit (TruSeq PE Cluster Kit v3 and TruSeq SBS Kit v3, Illumina) providing 2x100 bp paired-end reads. Libraries preparation and sequencing were performed at the GeT-PlaGe France Genomics sequencing platform (Toulouse, France). All the obtained data were submitted to the BBRIC Archive network (https://bbric-archive.toulouse.inra.fr/web/index.html) in Project Gpool.

Mapping and SNP calling

Reads from the 64 fastq files (4 lineages x 2 biological replicates x 4 lanes x 2 (paired-end)) were aligned to the *G. pallida* reference genome using Bowtie2 version 2.1.0 (Langmead *et al.* 2009; Langmead & Salzberg 2012) with default parameters. Duplicate reads were removed using Picard version 1.122.0 (http://broadinstitute.github.io/picard/) and remaining reads were realigned around indels using Realigner Target Creator and Indel Realigner from the Genome Analysis Toolkit, GATK version 2.8.0 (McKenna *et al.* 2010; DePristo *et al.* 2011; Van der Auwera *et al.* 2013). The 32 BAM files obtained were merged in a single mpileup file using SAMtools MPileup version 0.1.19 (Li *et al.* 2009) with minimum mapping quality and minimum base quality set to 20. The whole previous workflow was performed on the Galaxy platform (https://galaxyproject.org/, Blankenberg *et al.* 2010). The mpileup file was further processed to perform SNP calling and derive read counts for each alternative base, after discarding bases with a Base Alignment Quality score below 25. Genomic positions kept in the dataset had to show only two different bases across all the samples, however, the tri–allelic positions for which the third allele was represented by only one read were included in the analysis as bi-allelic SNPs (after filtering the third allele as a sequencing error). To evaluate the reproducibility of the sequencing results across the technical replicates (sequencing lanes), we carried out a Principal Component Analysis (PCA) based on the allele frequency counts (Fig. S1, Supporting information). A last filtering step based on the coverage and the minimum allele count (MAC) was performed: a SNP was kept in the dataset if i) it had a coverage of more than 30 reads and less than 300 reads (corresponding approximately to the 95% percentile of the empirical coverage distribution) in each sample and ii) the minor allele was represented by at least two reads in two different pool samples.

Genome scan for adaptive divergence and association with the virulent/avirulent status

To detect genomic signatures of selection, we used the package BayPass version 2.1 (Gautier 2015) that provides a reimplementation of the Bayesian hierarchical model initially proposed by Coop *et al.* (2010) and includes several extensions that improve accuracy and decision criteria. The underlying BayPass framework allows both to identify overly differentiated SNPs (candidate for adaptive selection) in a robust fashion, through the computation of the *XtX* genetic differentiation statistics (Günther & Coop 2013), and to perform genome-wide association with population-specific covariables. The underlying models explicitly account for the covariance structure among the population allele frequencies that originates from the shared history of the populations under study, through the estimation of the population covariance matrix Ω, which renders the identification of SNPs subjected to selection less sensitive to the confounding effect of demography (Bonhomme *et al.* 2010; Günther & Coop 2013). BayPass is generic enough to be suited for the analyses of data from experimental evolution in which the allele frequency covariance structure is simpler, and can handle data derived from Pool-Seq experiments (Gautier 2015).

The allele count dataset was analyzed under all the models implemented in BayPass with all the parameter set to default, considering the virulence/avirulence status (coded as a binary variable with value -1 and 1 respectively) of each sample for the association analysis. First, analysis under the core model allowed to estimate the *XtX* for each SNP that were calibrated after analyzing a pseudo-observed dataset (POD) simulated under the inference model with parameters set equal to those estimated in the real data. Second, we relied on the Bayes Factor (BF) calculated under the auxiliary covariate model to evaluate association of SNPs to the virulent/avirulent status of the lineages. The auxiliary covariate model involves

the introduction of a binary auxiliary variable to classify each locus as associated or not. This allows to easily compute Posterior Inclusion Probability (and BF) for each locus while explicitly accounting for multiple testing issues. For each SNP, the Bayes Factor (denoted BF_{mc} as in Gautier 2015) was expressed in deciban units (dB) via the transformation $10 \log_{10}$ (BF). As a decision rule, we then followed the popular Jeffreys' rule (Jeffreys 1961) that quantifies the strength of evidence (here in favor of association of the SNP with the covariable) as 'strong' when 10 dB < BF < 15 dB, 'very strong' when 15 dB < BF < 20 dB and 'decisive' when BF > 20 dB.

Three independent BayPass analyses were carried out for each model, giving different values to initial seed of the (pseudo-) Random Number Generator. Under the core model in particular, the posterior estimates of Ω were found almost identical with a FMD distance (Förstner & Moonen 2003) between each pair of matrices always lower than 0.01. For prioritization purposes, only SNPs that were overly differentiated if *XtX* > 1% POD significance threshold and if BF_{mc} > 20 in the three independent analyses were further considered as candidate.

As we were interested in identifying genomic regions involved in the adaptation to Iledher, we precisely had to consider only SNPs showing footprints of selection in the Iledher lineages (SMI and NI) and not in the Désirée lineages. It is in fact possible to pinpoint genomic regions involved in host adaptation (rather than resistance adaptation), which can occur both in nematode lineages having evolved on Iledher and in the ones having evolved on Désirée, as highlighted in Eoche-Bosy *et al.* (2016). For this purpose, we used the lnRH test (Kauer *et al.* 2003; Schlötterer & Dieringer 2005). LnRH is traditionally used for microsatellite datasets, but as it is not based on a particular mutation model (Kauer *et al.* 2003), it can also be applied to SNP datasets (Mc Evoy *et al.* 2006; Vasemägi *et al.* 2012).

This test, based on the assumption that markers linked to loci under selection will show reduced levels of diversity within populations (Schlötterer & Dieringer 2005), uses the expected heterozygosity H to compute the lnRH statistics. We merged allelic counts of biological replicates and derived from it allelic frequencies at each SNP in SMI, SMD, NI and ND. We computed the lnRH statistic for each locus in lineage pairs SMI/SMD and NI/ND by calculating the natural logarithm (ln) of the gene diversity ratio $[(1/(1-H_{lineage1}))^2-1] / [(1/(1-H_{lineage2}))^2-1]$. For lineages with monomorphic loci, one different allele was added to one individual, as null values of heterozygosity prevent the estimation of lnRH due to division by zero (Kauer *et al.* 2003). LnRH estimates were standardized to obtain a mean of 0 and a standard deviation of 1. As the lnRH is approximately normally distributed under the null hypothesis of neutrality (Schlötterer & Dieringer 2005), loci with lnRH values lower than -1.96 were considered outliers at the 0.05 threshold, indicating reduced variability in SMI and NI lineages as compared to SMD and ND, respectively. Only outliers in both lnRH pairwise comparisons were considered, and common outliers to BayPass and lnRH were retained to further investigation of their genic environment.

Genic environment of outlier loci

We searched for predicted genes located in a window of 120-kb around outlier loci (60-kb either side) in the annotated *G. pallida* genome. The choice of this value was based on the AFLP-based genetic linkage map of *G. rostochiensis* giving a physical:genetic distance ratio of 120 $kb.cM^{-1}$ (Rouppe van der Voort *et al.* 1999), as no data on the extent of recombination and linkage disequilibrium was available in *G. pallida*. As the majority of virulence factors identified in plant parasitic nematodes are effectors (Haegeman *et al.* 2012; Mitchum *et al.* 2013), we searched as a priority for genes coding for secreted proteins, *i.e.* harboring N-

terminal signal peptides in the predicted proteins, using SIGNALP v4.1 (Petersen *et al.* 2011). We also performed a BLAST search of the predicted genes against the annotated *G. rostochiensis* genome in order to potentially obtain more precise information on their functional annotation. Eves-van den Akker *et al.* (2016) identified in *G. rostochiensis* and subsequently in *G. pallida* genomes a dorsal gland promoter element motif, termed DOG Box, which may be a strong predictor of secretion, and thus likely effector function. We thus searched for the presence of the predicted genes identified around outlier loci in the *G. pallida* putative DOG effectors list established by Eves-van den Akker *et al.* (2016).

Results

Sequencing, mapping and SNP calling

Sequencing was carried out on duplicates of the lineages SMI, SMD, NI and ND. Despite the low amount of DNA used for each lineage, the generated sequencing data corresponded to the expectations from a quantitative and qualitative point of view. Sequencing produced two billion reads, *i.e*. 62.5 million reads/sample (biological replicate)/lane, and 76% mapped on the *G. pallida* reference genome, but 24% of these mapping reads mapped more than once on the genome. Duplicate filtering resulted in removing 13.5% of mapped reads. Remaining reads covered 95% of the ungapped assembly at an average depth of 34X/sample/lane. Processed mpileup contained 2,383,040 SNPs. PCA based on the allele frequency counts showed that the main axes of variation of genetic variability across the different samples were clearly associated with (i) the population origin and (ii) the virulence status. A very low variation was observed among the sequencing replicates in each pool sample. This prompted us to merge allele count data from the four sequencing replicates (lanes) for each of the eight pool samples (Fig. S1, Supporting information). The final dataset filtered on coverage and

MAC consisted of read count data for 1,631,158 SNPs in the eight different selected lineages, corresponding to a density of polymorphic sites of 16/kb on average.

Genome scan for adaptive divergence and association with the virulent/avirulent status

Analysis of the dataset under the BayPass core model allowed us to estimate the scaled covariance matrix of population allele frequencies Ω that quantifies the genetic relationship among each pairs of populations. The resulting estimates of Ω accurately reflected the known structure between samples, *i.e.* a clustering at the higher level by population geographical origin, then by the virulence status and finally by biological replicate within each lineage (Fig. 2). *XtX* for each SNP were also estimated and calibrated by analyses of a POD containing 1,600,000 SNPs. At the 1% POD significance threshold, about 33,000 SNPs were identified as overly differentiated (Fig. 3). However, analysis under the auxiliary covariate model drastically reduced this outlier list, as less than 400 had also a $BF_{mc} < 20$ (355, 361 and 357 SNPs in each analysis, respectively) (Fig. 3). Overall, 275 outliers were shared by the three analyses (outlier loci found in only one or two analyses actually exhibited *XtX* and/or BF_{mc} values close to the thresholds, which explains that they were not found in all analyses). Among these 275 SNPs showing an increase of genetic differentiation between Iledher and Désirée lineages, 31 of them also showed a decrease of genetic diversity in both SMI and NI lineages (Fig. 4) as identified by lnRH.

Genic environment of outlier loci

The 31 selected outlier loci were distributed on 23 different scaffolds. Among these outlier loci for which the genic environment has been investigated, three outliers were located on scaffolds which do not harbor any predicted gene, 16 were located in intergenic area and 12

were directly located into genes (Table S2, Supporting information). Among the latter, five were located in exons, and four of them corresponded to synonymous mutations. The outlier SNP located on the scaffold 1777 corresponded to a non-synonymous mutation that changes an arginine into a histidine in GPLIN_001438500, which is annotated as a transcribed hypothetical protein. Despite the fragmentation of the *G. pallida* genome in numerous scaffolds that precluded a clear analysis of the physical distances among most of the identified outliers, it appeared that several outlier loci were sometimes found in the same scaffold. The most significant was the scaffold 988 which contains four outlier SNPs close to each other (< 200 bp). Four other scaffolds (44, 85, 182 and 283) harbored outlier SNPs close to each other (< 200 bp) and a fifth scaffold (66) harbored also two outlier SNPs but that are 75 kb apart. The number of outlier SNPs found in a scaffold was not dependent on the size of this scaffold: for instance, scaffold 988, which is one of the smallest scaffold of interest identified, contains four outlier loci. Overall, 258 predicted genes were identified in a 120-kb window around the 31 outlier loci (Table S2, Supporting information). About 47% (121) of them have unknown function in *G. pallida*, but 15 harbored a signal peptide, indicating that they potentially encode for secreted proteins, and one, GPLIN_000314000, is similar to an effector in *G. rostochiensis* (Cotton *et al*. 2014). Fourteen predicted genes with known functions also harbored a peptide signal. Fifteen genes coding for proteins harboring a SPRY domain were found at the proximity of eight outlier loci, and three of them were paralog of SPRYSECs (Secreted protein with a SPRY domain), which are known in nematodes of the genus *Globodera* to be involved in pathogenicity but also in (a)virulence (Rehman *et al.* 2009; Sacco *et al.* 2009). Two of them, located on scaffolds 182 and 782, were paralog of RBP-1, the only virulence gene identified in *G. pallida* (Sacco *et al.* 2009; Carpentier *et al.* 2012). It is likely that some of the other genes coding for proteins harboring a SPRY domain could

actually be SPRYSECs, the absence of signal peptide being not ascertained as they are 5' truncated (N's region) in the reference genome. Other genes were also interesting as they encode proteins which have functions linked to *G. pallida* pathogenicity, e.g., cell wall modifying proteins, or they encode proteins which are known to be secreted by the dorsal pharyngeal gland of *G. pallida*. The pharyngeal glands are cells in which effectors are produced, and thus can be regarded as a toolbox for infection (Eves-van den Akker & Birch 2016). Cyst nematodes have two sets, subventral and dorsal: the former are primarily active while the nematode migrates through host tissue, while the latter are primarily active during the sedentary parasitic stages (Endo 1987; von Mende 1997; Davis *et al.* 2000). Some genes with unknown function in *G. pallida* had homologues with predicted function in *G. rostochiensis* genome, part of them being putatively paralog of SPRYSECs or involved in pathogenicity. Three predicted genes (GPLIN_000832500, GPLIN_001056700 and GPLIN_001258100) harbored DOG Boxes in their promoter region, two of them having unknown function and the third coding for a SPRYSEC protein.

Discussion

In this study, we investigated *Globodera pallida* genomic regions involved in the adaptation to the QTL $GpaV_{vrn}$, a resistance factor against this potato parasite, by performing a genome scan on Pool-Seq data derived from experimentally evolved lineages, adapted or not to the resistant potato cultivar Iledher.

Elucidating the molecular bases of virulence is a central challenge in nematology. So far, a few plant-nematode interactions have been studied to characterize the molecular determinants of (a)virulence. In *G. pallida*, only one virulence gene has been described (Sacco *et al.* 2009; Carpentier *et al.* 2012). *A priori* methods based on candidate genes to

identify new or unknown virulence genes are therefore not the most adapted ones at the moment. Our study is the first to exploit genome scan to target genetic bases of adaptation to plant resistance in nematode populations. We demonstrated in a previous study the feasibility of a genome scan approach on our specific biological materiel coming from short experimental evolution (Eoche-Bosy *et al.* 2016), which was achieved here by the identification of 275 outlier loci and 31 candidates of a strong interest among them, distributed on 23 scaffolds. Several genomic regions are therefore putatively linked to adaptation to the resistance of Iledher, however this number should be put in perspective with respects to the moderate quality of the *G. pallida* reference genome. In fact, the genome assembly is still relatively fragmented (6,873 scaffolds), which could suggest that different genomic regions identified as outliers in our study could in fact form only one or a few. Eves-van den Akker *et al.* (2016) highlighted that some effector islands identified in *G. rostochiensis* genome were split across different scaffolds in *G. pallida* genome. This prevents to make realistic assumptions on the number of genes that could be involved in the overcoming of Iledher resistance. However, we assume that only a few virulence genes should be involved as few resistance genetic factors are expected in Iledher because of the major effect of the QTL $GpaV_{vrn}$ which is present in the potato cultivar Iledher and the fast overcoming of this resistance observed in experimental evolution that support rather the view of a mono- or oligogenic resistance.

The moderate quality of the genome involved other limitations in mapping of sequencing reads, leading to the loss of a substantial part of the data. First, 24% of the sequencing reads did not map on the reference genome, while in the same time, the assembly contains 17% of N's and has a CEGMA completeness score of 74% for complete genes and 81% for partial genes (Parra *et al.* 2007; Eves-van den Akker *et al.* 2016). This suggests that a

large part of unmapped reads could actually belongs to the *G. pallida* genome, but corresponding sequences would be absent from the assemblage. These missing sequences could putatively comprise candidate genomic regions to adaptation. Second, heterozygosity of the reference genome is suspected, as about 24% of the sequencing reads mapped more than once on the genome, this hypothesis being supported by the difference between the length of the assembly (124.7 Mb) and the estimated genome size (100 Mb). Sequencing data mapping on these genomic regions were further discarded because of poor mapping score due to the multiple positions mapping, and once again, genomic information about these regions and their possible link to resistance adaptation were lost.

Pool-Seq is now commonly adopted in many studies, included population genomics studies (Rubin *et al.* 2010, 2012; Clément *et al.* 2013; Ferretti *et al.* 2013; Fisher *et al.* 2013), because it provides more accurate estimation of allele frequencies, at reduced sequencing and library preparation costs (Futschik & Schlötterer 2010; Zhu *et al.* 2012; Gautier *et al.* 2013; Rellstab *et al.* 2013; Schlötterer *et al.* 2014). Here, we emphasize the interest of using such an approach for population genomic studies of non-clonal microorganisms, as it allowed to increase the amount of DNA while keeping information about allele frequencies. The good quality of our results also relies on library preparation protocol, which fit the recommendations (Rhodes *et al.* 2014; Kofler *et al.* 2016). The TruSeq Nano DNA kit has been shown to be highly accurate and even some duplicates were obtained due to the PCR cycles, Kofler *et al.* (2016) showed that duplicates were also obtained with free-PCR library preparation kits. Nevertheless, Kofler *et al.* (2016) highlighted the superior impact of the genome quality over the library preparation protocol on the mapping quality. Numbers of individuals in pools and depth of coverage used have also been determined to improve sequencing results and allelic frequency estimations (Gautier *et al.* 2013; Kofler *et al.* 2016).

Consideration of a categorical population specific covariable in the genome scan allowed us to refine the list of outlier loci. Analysis of association further conducted by running the auxiliary covariate model allowed to retain only SNPs associated with the virulence status of the lineages, and not those corresponding to other selective pressures (e.g., local adaptation), which helped to reduce the risk of a misleading biological interpretation, a main limitation of genome scans (Pavlidis *et al.* 2012). Moreover, evaluating the reduction of diversity allowed us to refine the outlier loci list to those linked only to the adaptation to the resistant cultivar Iledher. A direct link between those candidate loci and the adaptation to the resistance cannot yet be done at this stage. Indeed, footprints of selection detected in lineages having evolved on Iledher might well be linked to adaptation to the plant resistance or to the plant itself (including all its genetic background). Also, at this stage, we are unable to definitively link the identified SNPs to the resistance factor $GpaV_{vrn}$ or to another resistance factor present in the genetic background of the cultivar Iledher. Although these different situations will only be deciphering by functional validation, there is a strong possibility that at least some of the candidate genomic regions identified in this study are involved in adaptation to Iledher resistance and in particular to its major resistance QTL $GpaV_{vrn}$.

Sixteen over the 31 outlier loci investigated for their genic environment have at least one gene coding for a secreted protein in their neighboring region (even if all secreted proteins are not effectors, all effectors are secreted protein) and several outliers are at the vicinity of genes coding for proteins specifically secreted in the nematode dorsal gland. Particularly, some of these secreted proteins are SPRYSECs effectors which act as a versatile protein-binding platform for the nematodes to target a wide range of host proteins during parasitism including plant resistance proteins (Rehman *et al.* 2009; Sacco *et al.* 2009; Diaz-Granados *et al.* 2016). The fact that a considerable part of the outlier loci are found near genes

476 coding for a SPRY domain containing protein or even in or at the vicinity of SPRYSECs
477 cannot be only explained by the huge size of this family gene or the prevalence of the SPRY
478 domain in the *G. pallida* genome. In fact, 299 SPRY domain containing proteins are present
479 in the *G. pallida* genome (which can be moreover cluster into islands), *i.e.* 1 for 334 kb, and
480 30 of them are SPRYSECs, *i.e.* 1 SPRYSEC for 3.33 Mb (Mei *et al.* 2015; Eves-van den
481 Akker *et al.* 2016). When looking at the genic environment of outlier loci, we explored a total
482 of 2 Mb of the genome and we identified 15 SPRY domain containing proteins, *i.e.* 1 for 133
483 kb, and 3 SPRYSECs, *i.e.* 1 for 660 kb. This is more than expected by chance in both cases
484 and therefore support the view that some SPRYSEC proteins should be well indeed involved
485 in the adaptation of *G. pallida* to Iledher.

486 It can be noticed that the lnRH test also identified, among the 275 outlier loci, six
487 SNPs showing a decrease of genetic diversity in both Désirée lineages (data not shown).
488 These loci were distributed on four scaffolds, different from those on which the 31 outliers
489 were located. Although we did not consider them in this study, those results could further be
490 used to study adaptation to the potato cultivar Désirée. Only one of the 13 microsatellite
491 markers identified as outliers by Eoche-Bosy *et al.* (2016) was located on the same scaffold as
492 one of the 31 outlier SNPs identified here, and no one was located on the same scaffold as the
493 six outlier SNPs involved in Désirée adaptation. The microsatellite marker Gp235 was indeed
494 located at about 150 bp from the outlier SNP identified here on the scaffold 216. The fact that
495 the other outlier microsatellites were not found on the same scaffold that outlier SNPs is not
496 surprising, due to the small number of microsatellites used and to the fragmentation of the
497 genome.

498 By identifying genomic regions putatively involved in the adaptation to the resistance
499 from *S. vernei*, the present study has taken a further step towards understanding and

identifying the determinants of virulence. In the aim of pinpointing, among the candidate loci, those actually involved in the adaptation to the potato cultivar Iledher, a first step of validation could consist of studying allele frequencies of candidate SNPs in natural populations showing different virulence level to Iledher, which could allow to validate some of them whose variations in allelic frequencies would correlate with variations in virulence level. Even if those loci are not the mutation responsible for the adaptation, they can be enough linked to it to be used as molecular tools to determine virulence allele frequencies in field populations before the deployment of resistant cultivars, and to study more accurately the potential fitness costs or benefits linked to the mutation from avirulence to virulence. Indeed, a recent study suggested that adaptation to Iledher involves an increase of fitness on a susceptible potato cultivar (Fournet *et al.* 2016). However, this study did not test for competition between avirulent and virulent individuals, because of the lack of molecular markers allowing to follow (a)virulence alleles. And it was shown in the *Potato Virus Y* that a cost of competitiveness could occur, even in absence of fitness cost in simple inoculation (Janzac *et al.* 2010). The identified outlier loci will also allow to target more precisely the best candidate genes involved in the adaptation, which will have to be functionally validated.

Acknowledgments

The authors gratefully acknowledge D. Mugniéry and M.C. Kerlan who took part in the experimental evolution, L. Renault, S. Bardou-Valette, C. Porte and D. Fouville who helped for the protocol elaboration and the pooled samples preparation, and M. Vidal for its help in libraries preparation. DEB is supported by the INRA department SPE and the Région Bretagne through a three year PhD grant.

References

Alenda C, Montarry J, Grenier E (2014) Human influence on the dispersal and genetic structure of French *Globodera tabacum* populations. *Infection, Genetics and Evolution*, **27**, 309-317.

Ayme V, Souche S, Caranta C *et al.* (2006) Different mutations in the genome-linked protein VPg of *Potato virus Y* confer virulence on the *pvr2*^{3} resistance in pepper. *Molecular Plant-Microbe Interactions*, **19**, 557-563.

Barbary A, Djian-Caporalino C, Palloix A, Castagnone-Sereno P (2015) Host genetic resistance to root-knot nematodes, *Meloidogyne* spp., in Solanaceae: from genes to the field. *Pest Management Science*, **71**, 1591–1598.

Bekal S, Domier LL, Gonfa B, Lakhssassi N, Meksem K, Lambert KN (2015). A SNARE-like protein and biotin are implicated in soybean cyst nematode virulence. *PLoS ONE*, **10**, e0145601.

Blankenberg D, Von Kuster G, Coraor N *et al.* (2010) Galaxy: a web-based genome analysis tool for experimentalists. *Current Protocols in Molecular Biology*, **89**, 19.10.1-19.10.21.

Bonhomme M, Chevalet C, Servin B *et al.* (2010) Detecting selection in population trees: the Lewontin and Krakauer test extended. *Genetics*, **186**, 241-262.

Carpentier J, Esquibet M, Fouville D, Manzanares-Dauleux MJ, Kerlan MC, Grenier E (2012) The evolution of the *Gp-Rbp-1* gene in *Globodera pallida* includes multiple selective replacements. *Molecular Plant Pathology*, **13**, 546-555.

Castagnone-Sereno P (2002) Genetic variability of nematodes: a threat to the durability of plant resistance genes? *Euphytica*, **124**, 193-199.

Clément JA, Toulza E, Gautier M *et al.* (2013) Private selective sweeps identified from next-generation pool-sequencing reveal convergent pathways under selection in two inbred *Schistosoma mansoni* strains. *PLoS Neglected Tropical Diseases*, **7**, e2591.

Coop G, Witonsky D, Rienzo A, Pritchard JK (2010) Using environmental correlations to identify loci underlying local adaptation. *Genetics*, **185**, 1411-1423.

Cotton JA, Lilley CJ, Jones LM *et al.* (2014) The genome and life-stage specific transcriptomes of *Globodera pallida* elucidate key aspects of plant parasitism by a cyst nematode. *Genome Biology*, **15**, R43.

Davis EL, Hussey RS, Baum TJ *et al.* (2000) Nematode parasitism genes. *Annual Review of Phytopathology*, **38**, 365-396.

DePristo MA, Banks E, Poplin R *et al.* (2011) A framework for variation discovery and genotyping using next-generation DNA sequencing data. *Nature Genetics*, **43**, 491-498.

Díaz JA, Nieto C, Moriones E, Truniger V, Aranda MA (2004) Molecular characterization of a *Melon necrotic spot virus* strain that overcomes the resistance in melon and nonhost plants. *Molecular Plant-Microbe Interactions*, **17**, 668-675.

Diaz-Granados A, Petrescu AJ, Goverse A, Smant G (2016) SPRYSEC effectors: a versatile protein-binding platform to disrupt plant innate immunity. *Frontiers in Plant Science*, **7**, 1575.

Djian-Caporalino C, Palloix A, Fazari A *et al.* (2014) Pyramiding, alternating or mixing: comparative performances of deployment strategies of nematode resistance genes to promote plant resistance efficiency and durability. *BMC Plant Biology*, **14**, 53.

Endo BY (1987) Ultrastructure of esophageal gland secretory granules in juveniles of *Heterodera glycines*. *Journal of Nematology*, **19**, 469-483.

Eoche-Bosy D, Gauthier J, Juhel AS *et al.* (2016). Experimentally evolved populations of the potato cyst nematode *Globodera pallida* allow the targeting of genomic footprints of selection due to host adaptation. *Plant Pathology*, doi: 10.1111/ppa.12646.

Eves-van den Akker S, Birch PR (2016) Opening the effector protein toolbox for plant-parasitic cyst-nematode interactions. *Molecular Plant*, **9**, 1451-1453.
Eves-van den Akker S, Laetsch DR, Thorpe P *et al.* (2016) The genome of the yellow potato cyst nematode, *Globodera rostochiensis*, reveals insights into the basis of parasitism and virulence. *Genome Biology*, **17**, 124.
Ferretti L, Ramos-Onsins SE, Pérez-Enciso M (2013) Population genomics from pool sequencing. *Molecular Ecology*, **22**, 5561-5576.
Fischer MC, Rellstab C, Tedder A *et al.* (2013) Population genomic footprints of selection and associations with climate in natural populations of *Arabidopsis halleri* from the Alps. *Molecular Ecology*, **22**, 5594-5607.
Förstner W, Moonen B (2003) A metric for covariance matrices. In: *Geodesy-The Challenge of the 3rd Millennium* (eds Grafarend EW, Krumm FW, Schwarze VS), pp. 299-309. Springer-Verlag, Berlin/Heidelberg, Germany.
Fournet S, Eoche-Bosy D, Renault L, Hamelin FM, Montarry J (2016) Adaptation to resistant hosts increases fitness on susceptible hosts in the plant parasitic nematode *Globodera pallida*. *Ecology and Evolution*, **6**, 2559-2568.
Fournet S, Kerlan MC, Renault L, Dantec JP, Rouaux C, Montarry J (2013) Selection of nematodes by resistant plants has implications for local adaptation and cross-virulence. *Plant Pathology*, **62**, 184-193.
Futschik A, Schlötterer C (2010) The next generation of molecular markers from massively parallel sequencing of pooled DNA samples. *Genetics*, **186**, 207-218.
Gautier M (2015) Genome-wide scan for adaptive differentiation and association analysis with population-specific covariables. *Genetics*, **201**, 1555-1579.
Gautier M, Foucaud J, Gharbi K *et al.* (2013) Estimation of population allele frequencies from next-generation sequencing data: pool-versus individual-based genotyping. *Molecular Ecology*, **22**, 3766-3779.
Green CD, Greet DN, Jones FGW (1970) The influence of multiple mating on the reproduction and genetics of *Heterodera rostochiensis* and *H. schachtii*. *Nematologica*, **16**, 309-326.
Günther T, Coop G (2013) Robust identification of local adaptation from allele frequencies. *Genetics*, **195**, 205-220.
Haegeman A, Mantelin S, Jones JT, Gheysen G (2012) Functional roles of effectors of plant-parasitic nematodes. *Gene*, **492**, 19-31.
Janzac B, Fabre F, Palloix A, Moury B (2009) Constraints on evolution of virus avirulence factors predict the durability of corresponding plant resistances. *Molecular Plant Pathology*, **10**, 599-610.
Janzac B, Montarry J, Palloix A, Navaud O, Moury B (2010) A point mutation in the polymeras *Potato Virus Y* confers virulence toward the *Pvr4* resistance of pepper and a high competitiveness cost in susceptible cultivar. *Molecular Plant-Microbe Interactions*, **23**, 823-830.
Jeffreys H (1961) *Theory of Probability*, 3rd edn. Oxford University Press, Oxford, UK.
Jones FGW (1950) Observations on the beet eelworm and other cyst-forming species of *Heterodera*. *Annals of Applied Biology*, **37**, 407-440.
Jones MGK, Northcote DH (1972) Nematode-induced syncytium – a multinucleate transfer cell. *Journal of Cell Science*, **10**, 789-809.
Kauer MO, Dieringer D, Schlötterer C (2003) A microsatellite variability screen for positive selection associated with the "Out of Africa" habitat expansion of *Drosophila melanogaster*. *Genetics*, **165**, 1137-1148.

Kofler R, Nolte V, Schlötterer C (2016) The impact of library preparation protocols on the consistency of allele frequency estimates in Pool-Seq data. *Molecular Ecology Resources*, **16**, 118-122.
Langmead B, Salzberg SL (2012) Fast gapped-read alignment with Bowtie 2. *Nature Methods*, **9**, 357-359.
Langmead B, Trapnell Cole, Pop M, Salzberg SL (2009) Ultrafast and memory-efficient alignment of short DNA sequences to the human genome. *Genome Biology*, **10**, R25.
Li H, Handsaker B, Wysoker A *et al.* (2009) The Sequence Alignment/Map format and SAMtools. *Bioinformatics*, **25**, 2078-2079.
Lozano-Torres JL, Wilbers RH, Gawronski P *et al.* (2012) Dual disease resistance mediated by the immune receptor Cf-2 in tomato requires a common virulence target of a fungus and a nematode. *Proceedings of the National Academy of Sciences of the United States of America*, **109**, 10119-10124.
Lozano-Torres JL, Wilbers RH, Warmerdam S *et al.* (2014) Apoplastic venom allergen-like proteins of cyst nematodes modulate the activation of basal plant innate immunity by cell surface receptors. *PLoS Pathogens*, **10**, e1004569.
Luikart G, England PR, Tallmon D, Jordan S, Taberlet P (2003) The power and promise of population genomics: from genotyping to genome typing. *Nature Reviews Genetics*, **4**, 981-994.
Mardis ER (2008) The impact of next-generation sequencing technology on genetics. *Trends in Genetics*, **24**, 133-141.
McDonald BA, Linde C (2002) Pathogen population genetics, evolutionary potential, and durable resistance. *Annual Review of Phytopathology*, **40**, 349-379.
McEvoy B, Beleza S, Shriver MD (2006) The genetic architecture of normal variation in human pigmentation: an evolutionary perspective and model. *Human Molecular Genetics*, **15**, R176-R181.
McKenna A, Hanna M, Banks E *et al.* (2010) The Genome Analysis Toolkit: A MapReduce framework for analyzing next-generation DNA sequencing data. *Genome Research*, **20**, 1297-1303.
Mei Y, Thorpe P, Guzha A *et al.* (2015) Only a small subset of the SPRY domain gene family in *Globodera pallida* is likely to encode effectors, two of which suppress host defences induced by the potato resistance gene *Gpa2*. *Nematology*, **17**, 409-424.
Meshi T, Motoyoshi F, Adachi A, Watanabe Y, Takamatsu N, Okada Y (1988) Two concomitant base substitutions in the putative replicase genes of tobacco mosaic virus confer the ability to overcome the effects of a tomato resistance gene, *Tm-1*. *EMBO Journal*, **7**, 1575-1581.
Mitchum MG, Hussey RS, Baum TJ *et al.* (2013) Nematode effector proteins: an emerging paradigm of parasitism. *New Phytologist*, **199**, 879-894.
Montarry J, Jan PL, Gracianne C *et al.* (2015) Heterozygote deficits in cyst plant-parasitic nematodes: possible causes and consequences. *Molecular Ecology*, **24**, 1654-1677.
Nicol JM, Turner SJ, Coyne DL, den Nijs L, Hockland S, Maafi ZT (2011) Current nematode threats to world agriculture. In: *Genomics and Molecular Genetics of Plant-Nematode Interactions* (eds Jones J, Gheysen G, Fenoll C), pp. 21-43. Springer, Dordrecht, The Netherlands.
Oerke EC, Dehne HW, Schönbeck F, Weber A (1994) *Crop production and crop protection: estimated losses in major food and cash crop*. Elsevier Science BV, Amsterdam, The Netherlands.

Parra G, Bradnam K, Korf I (2007) CEGMA: A pipeline to accurately annotate core genes in eukaryotic genomes. *Bioinformatics*, **23**, 1061-1067.
Pavlidis P, Jensen JD, Stephan W, Stamatakis A (2012) A critical assessment of storytelling: gene ontology categories and the importance of validating genomic scans. *Molecular Biology and Evolution*, **29**, 3237-3248.
Petersen TN, Brunak S, von Heijne G, Nielsen H (2011) SIGNALP 4.0: discriminating signal peptides from transmembrane regions. *Nature Methods*, **8**,785-786.
Picard D, Plantard O, Scurrah M, Mugniéry D (2004) Inbreeding and population structure of the potato cyst nematode (*Globodera pallida*) in its native area (Peru). *Molecular Ecology*, **13**, 2899-2908.
Plantard O, Porte C (2004) Population genetic structure of the sugar beet cyst nematode *Heterodera schachtii*: a gonochoristic and amphimictic species with highly inbred but weakly differentiated populations. *Molecular Ecology*, **13**, 33-41.
Rehman S, Postma W, Tytgat T *et al.* (2009) A secreted SPRY domain-containing protein (SPRYSEC) from the plant-parasitic nematode *Globodera rostochiensis* interacts with a CC-NB-LRR protein from a susceptible tomato. *Molecular Plant-Microbe Interactions*, **22**, 330-340.
Rellstab C, Zoller S, Tedder A, Gugerli F, Fischer MC (2013) Validation of SNP allele frequencies determined by pooled next-generation sequencing in natural populations of a non-model plant species. *PLoS ONE*, **8**, e80422.
Rhodes J, Beale MA, Fisher MC (2014) Illuminating choices for library prep: a comparison of library preparation methods for whole genome sequencing of *Cryptococcus neoformans* using Illumina HiSeq. *PLoS One*, **9**, e113501.
Rouppe van der Voort JNAM, van der Vossen E, Bakker E *et al.* (2000) Two additive QTLs conferring broad-spectrum resistance in potato to *Globodera pallida* are localized on resistance gene clusters. *Theoretical and Applied Genetics*, **96**, 654-661.
Rouppe van der Voort JNAM, van Eck HJ, van Zandvoort PM, Overmars H, Helder J, Bakker J (1999) Linkage analysis by genotyping of sibling populations: a genetic map for the potato cyst nematode constructed using a 'pseudo-F2' mapping strategy. *Molecular and General Genetics*, **261**, 1021–31.
Rubin CJ, Megens HJ, Barrio AM *et al.* (2012) Strong signatures of selection in the domestic pig genome. *Proceedings of the National Academy of Sciences of the United States of America*, **109**, 19529-19536.
Rubin CJ, Zody MC, Eriksson J *et al.* (2010) Whole-genome resequencing reveals loci under selection during chicken domestication. *Nature*, **464**, 587-591.
Sacco MA, Koropacka K, Grenier E *et al.* (2009) The cyst nematode SPRYSEC protein RBP-1 elicits Gpa2- and RanGAP2-dependent plant cell death. *PLoS Pathogens*, **5**, e1000564.
Schlötterer C, Dieringer D (2005) A novel test statistic for the identification of local selective sweeps based on microsatellite gene diversity. In: *Selective Sweep* (ed. Nurminsky D), pp. 55-64. Landes Bioscience, Georgetown, USA.
Schlötterer C, Tobler R, Kofler R, Nolte V (2014) Sequencing pools of individuals – mining genome-wide polymorphism data without big funding. *Nature Review Genetics*, **15**, 749-763.
Sobczak M, Golinowski W (2011) Cyst nematodes and syncytia. In: *Genomics and molecular genetics of plant-nematode interactions* (eds Jones JT, Gheysen G, Fenoil C), pp. 61-82. Springer, Dordrecht, The Netherlands.
Storz JF (2005) Using genome scans of DNA polymorphism to infer adaptive population divergence. *Molecular Ecology*, **14**, 671-688.

Triantaphyllou AC, Esbenshade PR (1990) Demonstration of multiple mating in *Heterodera glycines* with biochemical markers. *Journal of Nematology*, **22**, 452-456.
Van der Auwera GA, Carneiro MO, Hartl C *et al.* (2013) From FastQ data to high confidence variant calls: the Genome Analysis Toolkit best practices pipeline. *Current Protocols in Bioinformatics*, **43**, 11.10.1-11.10.33.
van Riel HR, Mulder A (1998) Potato cyst nematodes (*Globodera* species) in western Europe. In: *Potato Cyst Nematodes: Biology, Distribution and Control* (eds Marks RJ, Brodie BB), pp. 271-298. CAB International, Wallingford, UK.
Vasemägi A, Nilsson J, McGinnity P *et al.* (2012) Screen for footprints of selection during domestication/captive breeding of Atlantic Salmon. *Comparative and Functional Genomics*, **2012**, 628204.
von Mende N (1997) Invasion and migration behaviour of sedentary nematodes. In: *Cellular and Molecular Aspects of Plant–Nematodes Interactions* (eds Fenoll C, Grundler FMW, Ohl SA), pp. 51-64. Kluwer Academic Publishers, Dordrecht, The Netherlands.
Zhu Y, Bergland AO, González J, Petrov DA (2012) Empirical validation of pooled whole genome population re-sequencing in *Drosophila melanogaster*. *PLoS One*, **7**, e41901.

Data accessibility

Sequencing data were submitted to the BBRIC Archive network (https://bbric-archive.toulouse.inra.fr/web/index.html) in Project Gpool.

Author Contributions

SF performed the experimental evolution. DEB, ME, SF and JM performed the experiments according to a protocol elaborated jointly by DEB, EG and JM. OB performed the Illumina sequencing at the GeT-PlaGe platform (Toulouse, France). DEB, MG, FL and AB analyzed the data. DEB and JM wrote the text and prepared the figures. All authors edited the article and have approved the current version.

Supporting information

Additional supporting information may be found on the online version of this article.

Figure S1 Principal Component Analysis (PCA) of the sequencing data from eight *G. pallida* pools sequenced on four lanes (technical replicates), based on read counts at 2,383,040 SNPs.

Table S2 Putative functions of the predicted genes located in a 120-kb window centered on the 31 outlier loci on the *Globodera pallida* genome assembly version Gpal.v1.0 (Cotton *et al.* 2014).

Figure legends

Fig. 1 Selection of the four experimental *Globodera pallida* lineages. Nematode lineages were established from two French natural *G. pallida* populations, SM (near Saint-Malo, Brittany, north-western France) and N (from the island of Noirmoutier, western France), reared during eight successive cycles (*i.e.* eight generations) on the susceptible potato cultivar Désirée (D) and on the resistant cultivar Iledher (I). Each sample name indicates its geographical origin (SM for Saint-Malo and N for Noirmoutier) and the potato cultivar on which it evolved (I for Iledher and D for Désirée).

Fig. 2 Inferred relationship among the eight *G. pallida lineages* represented by a correlation plot and a hierarchical clustering tree derived from the matrix Ω estimated under the core model. Each sample name indicates its geographical origin (SM for Saint-Malo and N for Noirmoutier), the potato cultivar on which it evolved (I for Iledher and D for Désirée) and the replicate number (1 or 2).

Fig. 3 SNP *XtX* as a function of the BF_{mc} for association with the virulence status covariable, estimated in one of the three independent analyses. The vertical dotted line represents the 1% POD significance threshold (*XtX* = 14.0) and the horizontal dotted line represents the 20 dB threshold for BF_{mc}. Black dots represent the 275 outlier loci of interest (*i.e.* outliers for both *XtX* and BF_{mc} values) and red dots represent the 31 outlier loci of strong interest (*i.e.* outliers also identified with lnRH).

Fig. 4 Example of increase of genetic differentiation (represented as *XtX* estimates computed in BayPass across the whole dataset) and decrease of genetic diversity (represented as expected heterozygosity H in each lineages having evolved on Iledher) in a candidate genomic region. The scaffold represented is the scaffold 988 and the grey line indicates the location of the four outlier SNPs on the scaffold.

777 **Figure 1 – Eoche-Bosy et al.**

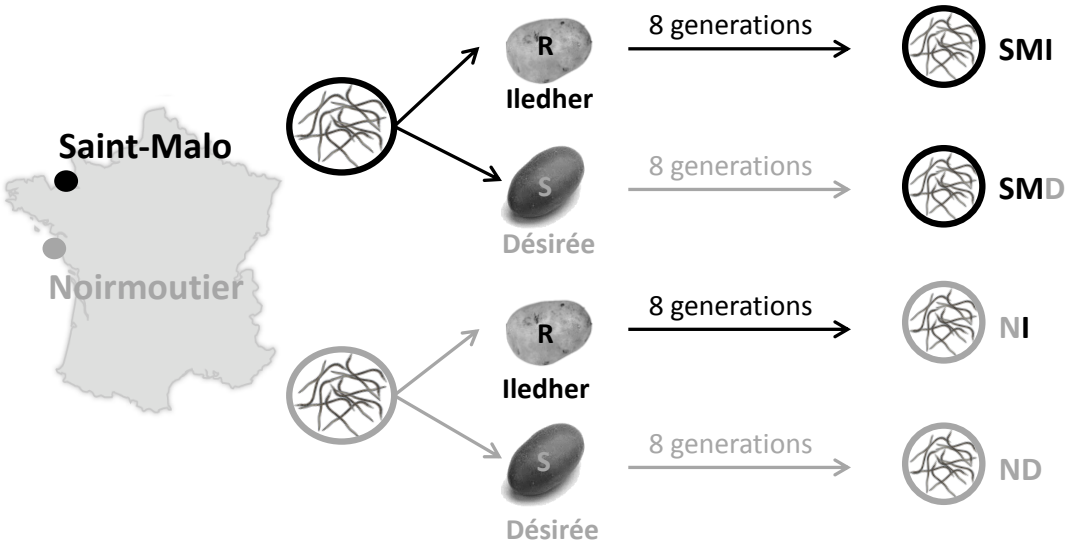

778

779 **Figure 2 – Eoche-Bosy et al.**

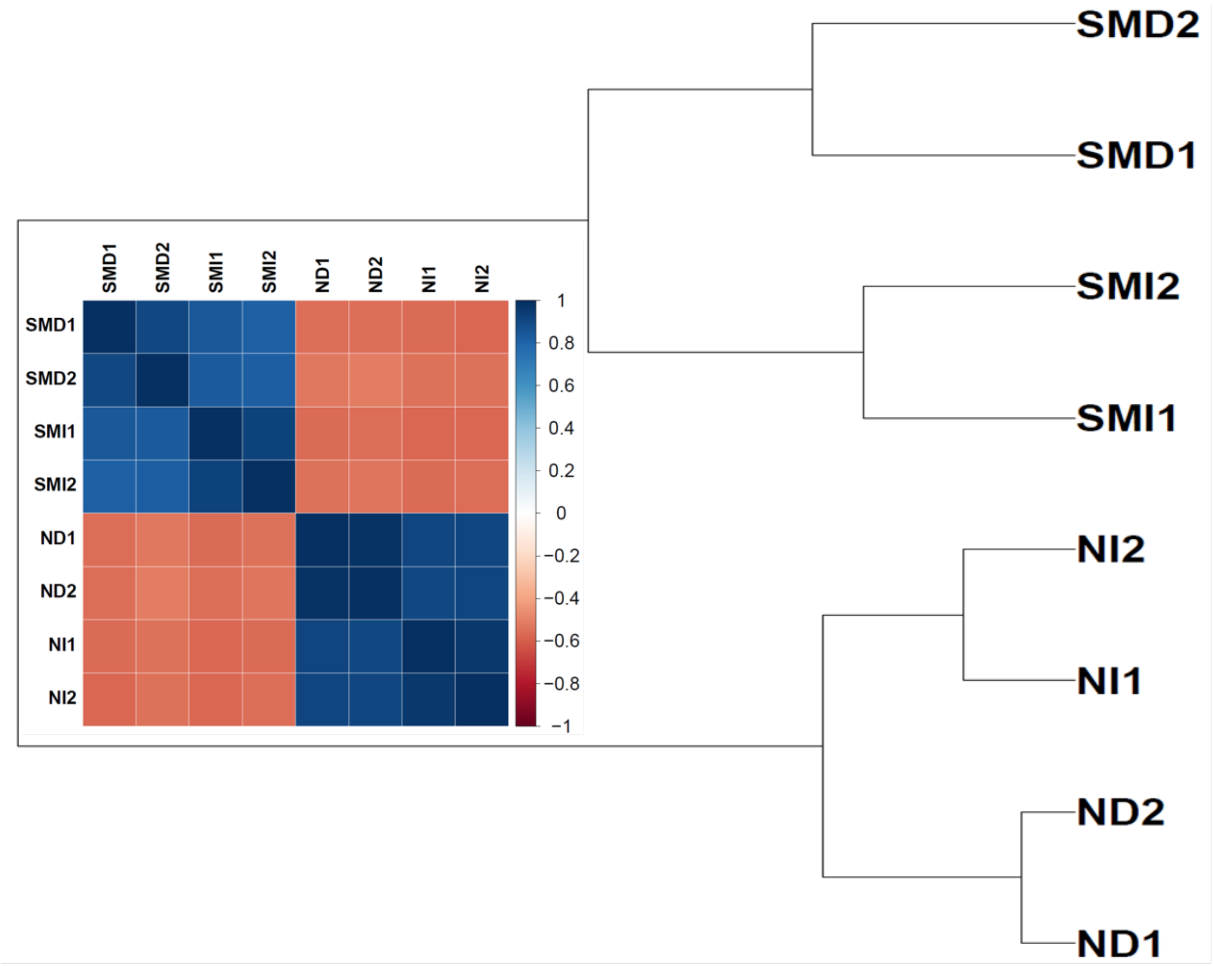

780

781 **Figure 3 – Eoche-Bosy et al.**

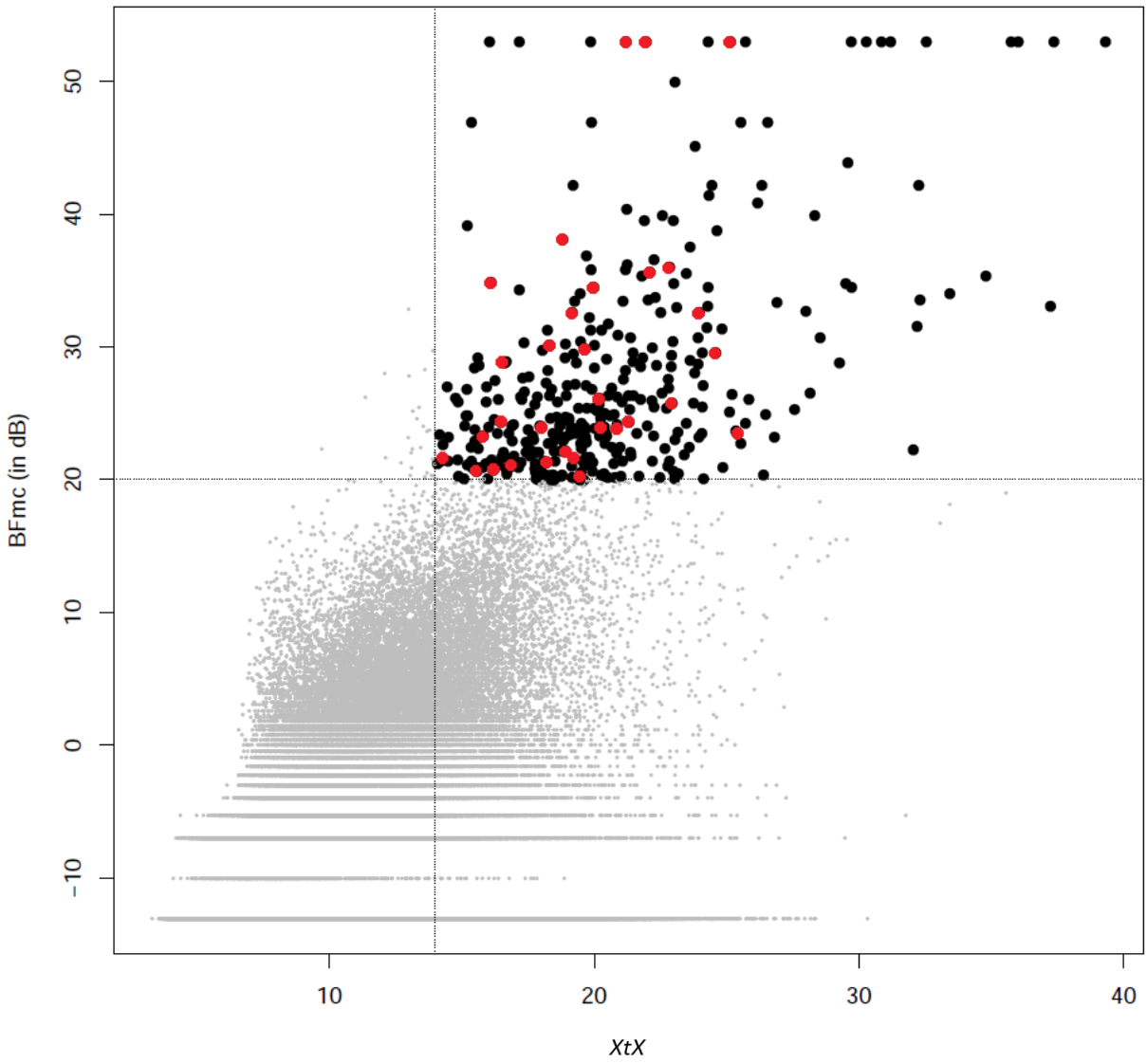

782

783 **Figure 4 – Eoche-Bosy et al.**

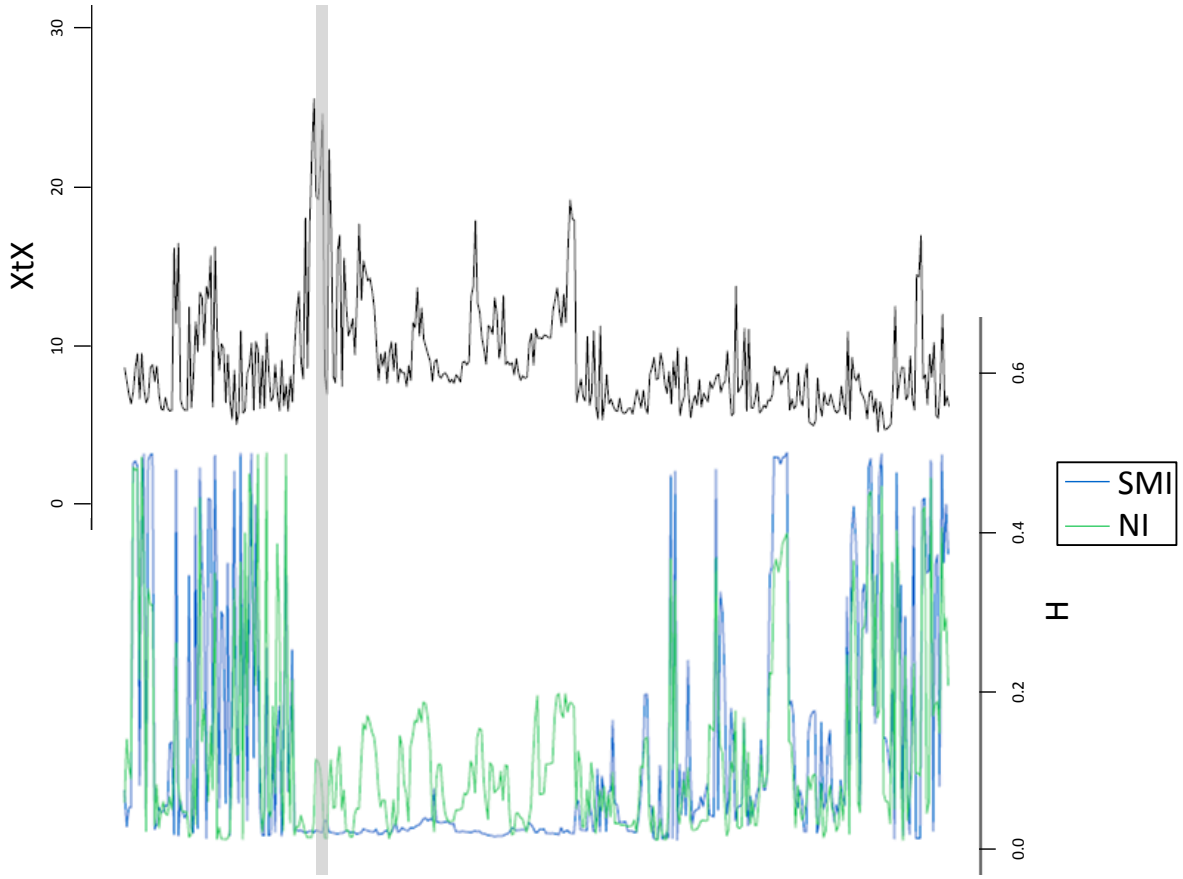

784

Supporting Information

Supplementary Figure S1

Principal Component Analysis (PCA) of the sequencing data from eight *G. pallida* pools sequenced on four different lanes (technical replicates), based on read counts at 2,383,040 SNPs. Each sample name indicates its geographical origin (SM for Saint-Malo and N for Noirmoutier), the potato cultivar on which it evolved (I for Iledher and D for Désirée), the number of the biological replicate (1 or 2) and the number of the lane (L) on which it has been sequenced. The first axis explains 32.61% of the variance and clusters the samples according to the population geographical origin. Even if the second and third axes explain a small part of the variance, *i.e.* 4.41% for PC2 and 4.22% for PCA3, they tend to cluster N and SM samples, respectively, according to their virulence status. Note however that for each of the eight pools, replicate sequenced on the first sequencing lane systematically depart from the three others. This patterns most probably results from a lower sequencing coverage for lane 1 (that was sequenced in 2x100 bp paired end) compared to the three others (that were sequenced in 2x125 bp paired-end)

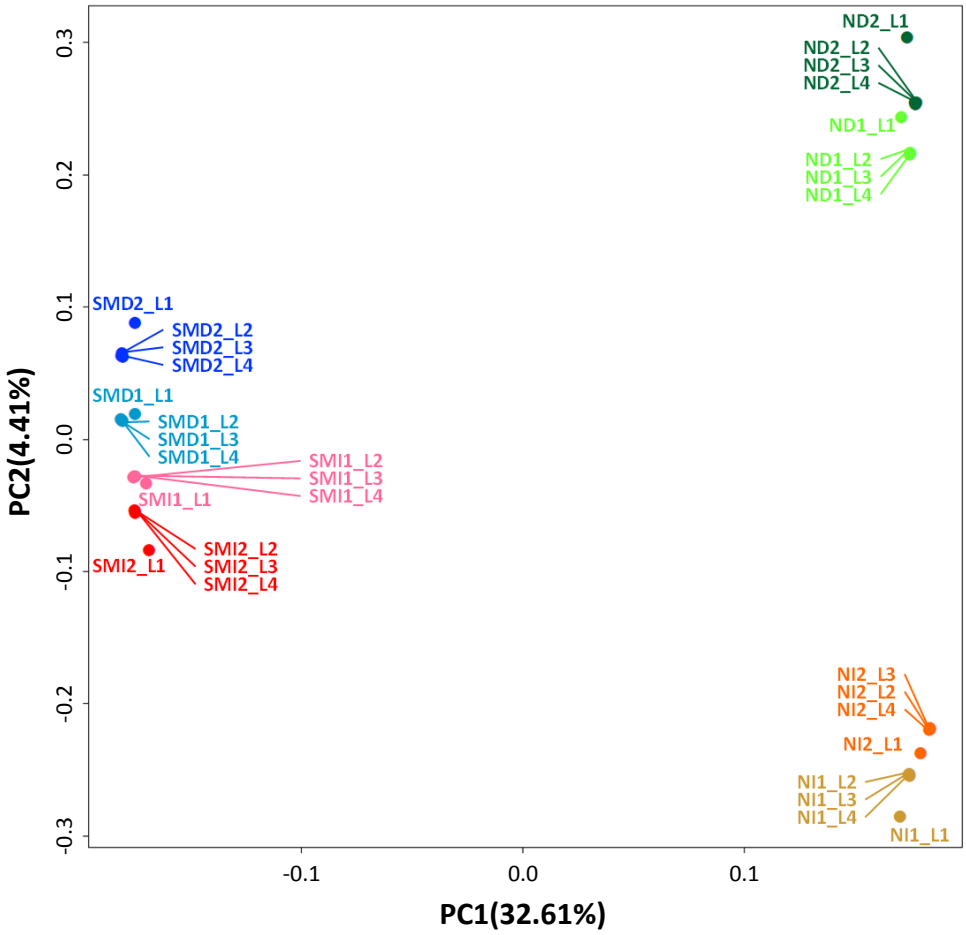

803

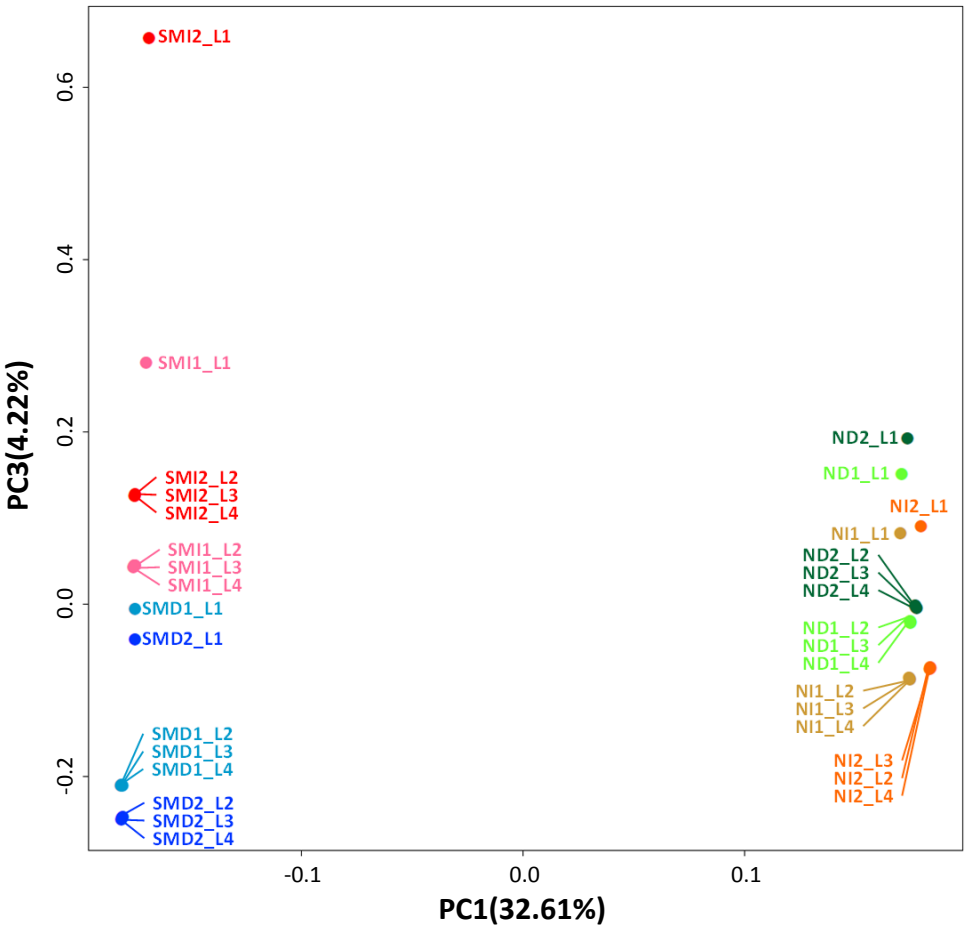
SMI2_L1
SMI1_L1
SMI2_L2
SMI2_L3
SMI2_L4
SMI1_L2
SMI1_L3
SMI1_L4
SMD1_L1
SMD2_L1
SMD1_L2
SMD1_L3
SMD1_L4
SMD2_L2
SMD2_L3
SMD2_L4
ND2_L1
ND1_L1
NI2_L1
NI1_L1
ND2_L2
ND2_L3
ND2_L4
ND1_L2
ND1_L3
ND1_L4
NI1_L2
NI1_L3
NI1_L4
NI2_L3
NI2_L2
NI2_L4
0.6
0.4
0.2
0.0
-0.2
PC3(4.22%)
-0.1
0.0
0.1
PC1(32.61%)

Supplementary Table S2

Putative functions of the predicted genes located in a 120-kb window centered on the 31 outlier loci on the *Globodera pallida* genome assembly version Gpal.v1.0 (Cotton *et al.* 2014). Relevant results of the BLAST search of the predicted genes against the annotated *G. rostochiensis* genome version nGr.v1.0 (Eves-van den Akker *et al.* 2016) are also shown. *: outlier SNP located in the gene, **: outlier SNP located in the exon.

Scaffold	Outlier locus	*Globodera pallida* genome				BLAST against *Globodera rostochiensis* genome	
		Gene ID	Location on the scaffold	Putative gene function	Peptide signal	Gene ID	Putative gene function
4	SNP_4_429075	GPLIN_0000030900	367074-371195	actin protein 6	no	GROS_g12208	spliceosome
		GPLIN_0000031000	371242-372608	nuclear Pore complex protein family member	no		
		GPLIN_0000031100	398790-400048	transcription initiation factor TFIID subunit	no		
		GPLIN_0000031200	403834-404255	beta 1 4 endoglucanase	no		
		GPLIN_0000031300*	428992-438734	transcribed hypothetical protein	no	GROS_g05341	magnesium ion transport; sodium ion transmembrane transport; integral to plasma membrane; cation channel activity
		GPLIN_0000031400	439019-440137	transcribed hypothetical protein	no		
		GPLIN_0000031500	441856-451123	cysteine synthase	no		
		GPLIN_0000031600	457740-458980	long chain fatty acid transport protein 4	no	GROS_g13363	fatty acid transport proteins
		GPLIN_0000031700	460388-460633	transcribed hypothetical protein	no		
		GPLIN_0000031800	462978-464011	beta 1,3 galactosyltransferase 2	no	GROS_g00450	galactosyltransferase
		GPLIN_0000031900	470256-470486	transcribed hypothetical protein	no		
		GPLIN_0000032000	471353-473130	transcribed hypothetical protein	no		
		GPLIN_0000032100	474046-474331	transcribed hypothetical protein	no	GROS_g10714	protein binding; stress-activated map kinase interacting protein 1 (SIN1)

		GPLIN_000149900	243326-245017	solute carrier family 35 member B1	yes	GROS_g02151	transport
		GPLIN_000150000	245308-249627	mitogen activated protein kinase kinase kinase	no	GROS_g02150	MAPK signaling pathway
		GPLIN_000150100	251276-252209	superoxide dismutase (Cu Zn)	yes	GROS_g02149	peroxisome
		GPLIN_000150200	252398-253488	transcribed hypothetical protein	no	GROS_g02148	transmembrane
		GPLIN_000150300	254217-258092	transcribed hypothetical protein	no	GROS_g02146	RNA transport; negative regulation of DNA damage checkpoint
		GPLIN_000150400	258929-261360	T complex protein 1 subunit epsilon	no	GROS_g02145	cytoskeleton organization; posttranslational protein folding
		GPLIN_000150500	261650-263494	transcribed hypothetical protein	no	GROS_g14282	metabolism of xenobiotics by cytochrome P450
		GPLIN_000150600	263679-265256	protein vertebrate galectins	yes	GROS_g02143	galactose binding; signal transducer activity
		GPLIN_000150700	265891-266885	N alpha acetyltransferase 20	no	GROS_g02141	endocytosis
		GPLIN_000150800	266955-269813	transcribed hypothetical protein	no	GROS_g02140	protein homodimerization activity
25	SNP_25_304232	GPLIN_000150900	269952-271262	transcribed hypothetical protein	no	GROS_g02139	transmembrane
		GPLIN_000151000	271403-272406	transcribed hypothetical protein	no		
		GPLIN_000151100	273509-275230	fasciculation and elongation protein zeta 2	no	GROS_g02137	axon guidance
		GPLIN_000151200	275973-277291	protein kinase domain containing protein, ck worm protein kinase	no		
		GPLIN_000151300	279494-280946	calmodulin	no	GROS_g02136	calmodulin
		GPLIN_000151400	284171-284443	transcribed hypothetical protein	no		
		GPLIN_000151500	299966-302277	cyclin-dependent kinase inhibitor	no		
		GPLIN_000151600*	303454-310418	exportin 7	no	GROS_g02131	nuclear export signal receptor activity; protein export from nucleus; nuclear pore
		GPLIN_000151700	310648-311820	glutaredoxin 3	no	GROS_g02130	glutaredoxin-3
		GPLIN_000151800	313085-314369	transcribed hypothetical protein	no		
		GPLIN_000151900	315934-316953	transcribed hypothetical protein	no	GROS_g02129	transmembrane
		GPLIN_000152000	317223-324014	DEAD Box protein	no	GROS_g02128	ATP catabolic process

		GPLIN_000152100	328566-329000	transcribed hypothetical protein	no		
		GPLIN_000152200	329118-330907	transcribed hypothetical protein	no	GROS_g02126	chromatin binding
		GPLIN_000152300	335501-336396	immunoglobulin i set domain containing protein	yes	GROS_g02125	transmembrane
		GPLIN_000152400	336805-340764	transcribed hypothetical protein	no	GROS_g02124	Golgi apparatus
		GPLIN_000152500	341193-341716	transcribed hypothetical protein	no		
		GPLIN_000232300	163392-163732	transcribed hypothetical protein	no		
		GPLIN_000232400	168518-169562	transcribed hypothetical protein	yes	GROS_g04085	signal peptide
		GPLIN_000232500	169991-170378	transcribed hypothetical protein	no		
		GPLIN_000232600	171849-174837	transcribed hypothetical protein	yes	GROS_g04087	signal peptide
		GPLIN_000232700	180474-181761	phosphatidylcholine:ceramide	no	GROS_g04089	sphingolipid metabolism
		GPLIN_000232800	183265-184828	60S ribosomal protein L4	no	GROS_g04090	cell wall modification; ribosomal protein L1e signature
		GPLIN_000232900	184937-188002	palmitoyltransferase ZDHHC2	no	GROS_g04091	proteinS-acyltransferase
		GPLIN_000233000	196131-198830	transcribed hypothetical protein	no	GROS_g11539	Transmembrane
		GPLIN_000233100	198931-200169	transcribed hypothetical protein	no		
		GPLIN_000233200	200212-201447	transcribed hypothetical protein	no		
	SNP_44_221212	GPLIN_000233300	201499-202356	transcribed hypothetical protein	no		
44		GPLIN_000233400	202494-203706	transcribed hypothetical protein	no		
	SNP_44_221214	GPLIN_000233500	203859-205030	worm specific Argonaute NRDE 3	no		
		GPLIN_000233600	205120-205935	transcription factor TFIID, C-terminal DNA glycosylase, N-terminal	no		
		GPLIN_000233700	206066-211386	transcribed hypothetical protein	no		
		GPLIN_000233800	211708-212533	transcribed hypothetical protein	no		
		GPLIN_000233900	212735-214448	transcribed hypothetical protein	no		

		GPLIN_000234000	221431-221718	transcribed hypothetical protein	no		
		GPLIN_000234100	221849-222821	polynucleotide kinase 3' phosphatase	no		
		GPLIN_000234200	255627-261288	macrophage erythroblast attacher	yes	GROS_g03239	CTLH/CRA C-terminal to LisH motif domain; actin cytoskeleton; negative regulation of myeloid cell apoptotic process
		GPLIN_000234300	264876-267441	mitochondrial processing peptidase beta subunit	no	GROS_g03235	insulinase (peptidase family M16)
		GPLIN_000234400	268640-269749	U1 small nuclear ribonucleoprotein A	no	GROS_g03234	regulation of alternative nuclear mRNA splicing, via spliceosome
		GPLIN_000234500	270323-271985	guanine nucleotide binding protein subunit	no	GROS_g03233	small ribosomal subunit; ion channel inhibitor activity
		GPLIN_000234600	272436-274181	transcribed hypothetical protein	no	GROS_g03232 / GROS_g03238	mitochondrion; negative regulation of synaptic transmission, glutamatergic / ATP catabolic process; adenosinetriphosphatase
		GPLIN_000234700	274837-276164	receptor expression enhancing protein 5	no	GROS_g03231	protein binding
		GPLIN_000234800	276256-277074	G protein coupled receptor associated sorting	no		
		GPLIN_000234900	277860-282940	4 aminobutyrate aminotransferase, mitochondrial	no	GROS_g03230 / GROS_g03230	beta-Alanine metabolism / beta-Alanine metabolism
		GPLIN_000311400	1-3999	transcribed hypothetical protein	no	GROS_g12784	signal peptide
		GPLIN_000311500	19418-20911	transcribed hypothetical protein	no	GROS_g14260	RBP-4 protein [*G. pallida*]
		GPLIN_000311600	30359-32404	transcribed hypothetical protein	no	GROS_g14196	RBP-4 protein [*G. pallida*]; secreted SPRY domain-containing protein 18 [*G. rostochiensis*]
	SNP_66_55507	GPLIN_000311700	36477-37252	transcribed hypothetical protein	no		
		GPLIN_000311800	45302-45915	transcribed hypothetical protein	no	GROS_g04023	riboflavin metabolism
66		GPLIN_000311900	46907-48176	BTB:POZ domain containing protein 3	yes	GROS_g14128	RBP-1 protein, partial [*G. pallida*]
	SNP_66_131126	GPLIN_000312000	49696-50448	transcribed hypothetical protein	no	GROS_g14136	RBP-4 protein [*G. pallida*]; transmembrane
		GPLIN_000312100	53144-55475	protein containing SPRY domain	no	GROS_g14278	RBP-1 protein [*G. pallida*]
		GPLIN_000312200	57585-58590	transcribed hypothetical protein	no	GROS_g11189	peptidase family M41
		GPLIN_000312300	66233-69356	protein containing SPRY domain	no	GROS_g14130	truncated secreted SPRY domain-containing protein 15, partial [*G. rostochiensis*]; signal peptide

		GPLIN_000312400	71724-72660	transcribed hypothetical protein	no		
		GPLIN_000312500	92978-94740	protein containing SPRY domain	no	GROS_g14278	RBP-1 protein [*G. pallida*]
		GPLIN_000312600	95754-96913	protein containing SPRY domain	no	GROS_g14287	truncated secreted SPRY domain-containing protein 15, partial [*G. rostochiensis*]
		GPLIN_000312700	107749-107949	EF-hand 2 domain containing protein	no	GROS_g14281	EF-hand calcium-binding domain.
		GPLIN_000312800	111831-112806	transcribed hypothetical protein	no	GROS_g05729	protein SAX-7 ; transmembrane
		GPLIN_000312900	112920-115358	group 1 glycosyl transferase	no	GROS_g01727	glycosyl transferases group 1
		GPLIN_000313000	119091-120888	transcribed hypothetical protein	no		
		GPLIN_000313100	124022-124830	transcribed hypothetical protein	no		
		GPLIN_000313200* (SNP_66_131126)	129063-137156	Sensory AXon guidance family member (sax 7)	no	GROS_g05729	protein SAX-7; sensory AXon guidance ; transmembrane
		GPLIN_000313300	139135-140624	transcribed hypothetical protein	no		
		GPLIN_000313400	142713-144269	transcribed hypothetical protein	no		
		GPLIN_000313500	145772-146732	transcribed hypothetical protein	no	GROS_g13276	signal peptide
		GPLIN_000313600	154523-157608	beta 1,4 endoglucanase (cell wall modifying protein); putative GH5 cellulase (cellulose degradation)	yes	GROS_g07446	beta-1,4-endoglucanase, partial; cellulase
		GPLIN_000313700	158653-160495	transcribed hypothetical protein	no	GROS_g02105	poly(A) polymerase central domain; nuclear mRNA splicing, via spliceosome
		GPLIN_000313800	167056-168124	transcribed hypothetical protein	no	GROS_g07447	EB module
		GPLIN_000313900	168962-169322	transcribed hypothetical protein	no	GROS_g01126	transmembrane
		GPLIN_000314000	183685-184563	transcribed hypothetical protein, similar to *G. rostochiensis* effector 1106	yes	GROS_g14309	signal peptide; 1106 effector family [*G. rostochiensis*]
85	SNP_85_126066	GPLIN_000382000	67804-68769	glutaminyl peptide cyclotransferase	no	GROS_g07374	signal peptide; peptidase M28 domain containing protein [*Haemonchus contortus*]
		GPLIN_000382100	84608-86814	transcribed hypothetical protein	no	GROS_g14124	RBP-4 protein [*G. pallida*]
	SNP_85_126206	GPLIN_000382200	94832-100930	zinc finger protein	no	GROS_g11336	zinc finger protein [*Loa loa*]
		GPLIN_000382300	110433-110747	transcribed hypothetical protein	no		

		GPLIN_000382400	120748-122590	BTB:POZ domain containing protein 3	no	GROS_g14193	truncated secreted SPRY domain-containing protein 15, partial [*G. rostochiensis*]
		GPLIN_000382500	126792-129853	SPla RYanodine receptor SPRY	no	GROS_g14163	RBP-4 protein [*G. pallida*]
		GPLIN_000382600	142203-143446	transcribed hypothetical protein	no		
		GPLIN_000382700	143942-144891	transcribed hypothetical protein	no		
		GPLIN_000382800	151467-154962	E9 protein	no	GROS_g14123	signal peptide
		GPLIN_000382900	164278-168506	glutathione synthetase	no	GROS_g05390 / GROS_g13797	glutathione synthetase-like [*Maylandia zebra*] / glutathionesynthase; signal peptide
		GPLIN_000383000	169444-172268	Guanine nucleotide binding protein G(o) subunit	no	GROS_g05389	guanine nucleotide-binding protein alpha-3 subunit [*Brugia malayi*]
		GPLIN_000383100	174565-177704	ODR 3	no	GROS_g05389	guanine nucleotide-binding protein alpha-3 subunit [*B. malayi*]
		GPLIN_000383200	179602-190327	guanine nucleotide exchange factor for Ras	no	GROS_g05388	regulation of Ral GTPase activity
111	SNP_111_140151	GPLIN_000450000	79896-81897	UDP glucuronosyltransferase	yes	GROS_g09337	integral to plasma membrane
		GPLIN_000450100	94652-95140	hypothetical protein	no		
		GPLIN_000450200	98715-99013	transcribed hypothetical protein	no		
		GPLIN_000450300	120569-121060	hypothetical protein	no		
		GPLIN_000450400	126241-129974	protein containing SPRY domain	no	GROS_g14195	dendrite morphogenesis, truncated secreted SPRY domain-containing protein 15, partial [*G. rostochiensis*]
		GPLIN_000450500	132676-135723	inversin protein alternative, ankyrin repeat protein	no	GROS_g14192	protein binding
		GPLIN_000450600	133821-134846	BTB:POZ domain containing protein 3	no	GROS_g14195	dendrite morphogenesis, truncated secreted SPRY domain-containing protein 15, partial [*G. rostochiensis*]
		GPLIN_000450700	138326-138779	transcribed hypothetical protein	no		
		GPLIN_000450800	138941-139562	Nematode AStacin protease family member	no	GROS_g07422	molting cycle, collagen and cuticulin-based cuticle; Astacin
		GPLIN_000450900	144927-150255	NAD kinase domain containing protein 1	no	GROS_g12807 / GROS_g12808	NAD metabolic process / mRNA surveillance pathway
		GPLIN_000451000	153798-155515	transcribed hypothetical protein	no		

		GPLIN_000451100	156162-159524	Amino Acid Transporter family member (aat 5)	no	GROS_g12805 / GROS_g00275	transmembrane transport / protein digestion and absorption
		GPLIN_000451200	160262-161491	cyclin B	no	GROS_g04262	microtubule cytoskeleton
		GPLIN_000451300	162184-162860	transcribed hypothetical protein	no	GROS_g04261	bifunctional 3 -phosphoadenosine 5 -phosphosulfate synthase [*Ascaris suum*]
		GPLIN_000451400	163767-166872	serine:threonine protein phosphatase 5	no	GROS_g04260	transcription, DNA-dependent
		GPLIN_000451500	168900-173567	transcribed hypothetical protein	no	GROS_g04258	protein binding
		GPLIN_000451600	174095-175144	40S ribosomal protein S26	no	GROS_g04257	RNA metabolic process
		GPLIN_000451700	175416-177669	transcribed hypothetical protein	no	GROS_g04256	transmembrane
		GPLIN_000451800	177949-181975	DNA replication licensing factor MCM6	no	GROS_g04255	cell cycle - yeast
		GPLIN_000451900	182477-187262	SWI:SNF complex subunit SMARCC2	no	GROS_g04254	ATP catabolic process
		GPLIN_000452000	187774-189157	DNA replication complex GINS protein SLD5	no	GROS_g04253	nucleoplasm
		GPLIN_000452100	192011-196045	transcribed hypothetical protein	no	GROS_g04252	transmembrane
		GPLIN_000452200	197876-201179	transcribed hypothetical protein	no	GROS_g10891	galactosyl beta-1,3 N-acetylgalactosamine beta-1,3-glucuronosyltransferase activity
123	SNP_123_97233	GPLIN_000482300	35198-37842	KH domain containing protein	no	GROS_g06084	nematode larval development; masculinization of hermaphroditic germ-line
		GPLIN_000482400	59414-60834	transcribed hypothetical protein	no		
		GPLIN_000482500	61285-62959	nematode cuticle collagen N terminal domain	no	GROS_g11113	larval development ; transmembrane
		GPLIN_000482600	72586-74133	transcribed hypothetical protein	yes		
		GPLIN_000482700	79061-79808	transcribed hypothetical protein	no	GROS_g13551	signal peptide
		GPLIN_000482800	85115-87297	mucosa associated lymphoid tissue lymphoma	no		
		GPLIN_000482900	87613-89268	mucosa associated lymphoid tissue lymphoma	no		
		GPLIN_000483000	89592-91491	mucosa associated lymphoid tissue lymphoma	no	GROS_g11117	ubiquitin-protein ligase activity; peptidase activity
		GPLIN_000483100	98509-100826	sucrose hydrolase	no	GROS_g11374	beta-fructofuranosidase; signal peptide

		GPLIN_000483200	101689-102752	tail length tape measure protein	no		
		GPLIN_000483300	103018-107209	beta fructofuranosidase; secreted GH32 fructosidase	yes	GROS_g11397	beta-fructofuranosidase; plant-type cell wall modification
		GPLIN_000483400	108777-111065	transcribed hypothetical protein	yes		
		GPLIN_000483500	112509-112790	transcribed hypothetical protein	no		
		GPLIN_000483600	117038-117476	transcribed hypothetical protein	yes		
		GPLIN_000483700	119298-120112	mps one binder kinase activator 3 like	no	GROS_g09711	neuronal cell body; perinuclear region of cytoplasm; microtubule cytoskeleton organization
		GPLIN_000483800	120304-121636	ubiquitin interacting motif	no	GROS_g09712	perinuclear region of cytoplasm
		GPLIN_000483900	121782-123696	ATP synthase subunit beta, mitochondrial	no	GROS_g09713	oxidative phosphorylation
		GPLIN_000484000	123896-127752	protein arginine N methyltransferase 5	no	GROS_g09714	protein ubiquitination; negative regulation of mitotic cell cycle
		GPLIN_000484100	128956-130197	tryptophanyl tRNA synthetase	no		
		GPLIN_000484200	137371-139503	transcribed hypothetical protein	no	GROS_g09707	transmembrane
		GPLIN_000484300	141658-142945	receptor type tyrosine protein phosphatase eta	no	GROS_g05032	protein tyrosine phosphatase activity; salicylic acid mediated signaling pathway
		GPLIN_000484400	148275-154307	transcribed hypothetical protein	no	GROS_g05028	glycerophospholipid metabolism; phosphatidylcholine metabolic process; signal peptide
		GPLIN_000484500	154735-155098	transcribed hypothetical protein	no		
		GPLIN_000484600	155919-159554	mitotic checkpoint serine:threonine protein	no	GROS_g04287 / GROS_g05027	regulation of chromosome segregation; positive regulation of intrinsic apoptotic signaling pathway / mitotic cell cycle spindle assembly checkpoint
182	SNP_182_414	GPLIN_000626500	1034-2234	protein containing SPRY domain	no	GROS_g14241	regulation of Ran GTPase activity; RBP-1 protein [G.*pallida*]
		GPLIN_000626600	4596-5610	transcribed hypothetical protein	no		
		GPLIN_000626700	9510-11116	protein containing SPRY domain	no	GROS_g14184	regulation of Ran GTPase activity; RBP-4 protein [*G. pallida*]
	SNP_182_557	GPLIN_000626800	13854-21499	protein containing SPRY domain	no	GROS_g14196	cytoplasmic microtubule; RBP-4 protein [*G. pallida*]
		GPLIN_000626900	23491-25804	protein containing SPRY domain	no	GROS_g14195	truncated secreted SPRY domain-containing protein 15, partial [*G. rostochiensis*]
		GPLIN_000627000	27744-30562	transcribed hypothetical protein	no		

		GPLIN_000627100	41665-44164	paralog of RBP-1 protein	yes	GROS_g14256	ran GTPase binding; RBP-1 protein, partial [*G. pallida*]
		GPLIN_000627200	45726-46823	60S acidic ribosomal protein P1	no	GROS_g01370	ribosome
		GPLIN_000627300	49760-52726	transcribed hypothetical protein	no		
		GPLIN_000627400	55950-61422	serpin protein	yes	GROS_g09868	extracellular space
		GPLIN_000691700	593-1233	transcribed hypothetical protein	no		
		GPLIN_000691800	3867-5051	dorsal gland cell specific expression protein	no	GROS_g14298	dorsal gland cell-specific expression protein [*Heterodera avenae*]
		GPLIN_000691900	9497-12258	mimitin, mitochondrial	no	GROS_g05274	NADH ubiquinone oxidoreductase subunit NDUFA12
		GPLIN_000692000	13158-18286	succinyl CoA:3 ketoacid coenzyme A transferase	no	GROS_g05277 / GROS_g02487	butanoate metabolism / butanoate metabolism
		GPLIN_000692100	18536-19094	histone cluster 2, H3c2	no	GROS_g05278	protein complex
		GPLIN_000692200	19401-19965	H2A histone family, member X	no	GROS_g10756	positive regulation of DNA repair
		GPLIN_000692300	21646-27499	transcribed hypothetical protein	no	GROS_g02034	small GTPase mediated signal transduction
216	SNP_216_53947	GPLIN_000692400	27752-30375	transcribed hypothetical protein	no		
		GPLIN_000692500*	31556-57322	copine domain containing protein 2	no	GROS_g02032	plasma membrane
		GPLIN_000692600	57566-59215	transcribed hypothetical protein	no	GROS_g02032	plasma membrane
		GPLIN_000692700	66169-72222	solute carrier family 23	no	GROS_g02031 / GROS_g03645	nucleobase transport / plasma membrane
		GPLIN_000692800	78865-80575	serine:arginine rich splicing factor 4	no	GROS_g02030	mitosis
		GPLIN_000692900	83168-85506	T complex protein 1 subunit gamma	no	GROS_g02028	extracellular vesicular exosome
		GPLIN_000693000	85945-87738	T complex protein 1 subunit gamma	no	GROS_g02028	extracellular vesicular exosome
		GPLIN_000693100	88182-90397	heterogeneous nuclear ribonucleoprotein A1	no	GROS_g02026	spliceosome
		GPLIN_000693200	91404-93983	transcribed hypothetical protein	no	GROS_g02025	phosphatidylinositol-4,5-bisphosphate4-phosphatase.

		GPLIN_000693300	95369-98967	transcribed hypothetical protein	no	GROS_g02024	plasmin
		GPLIN_000693400	100056-103180	nicotinic acetylcholine receptor non alpha	yes	GROS_g02022	response to inorganic substance
		GPLIN_000693500	104161-105279	transcribed hypothetical protein	no	GROS_g02021	hypothetical protein Y032_0018g3584 [*Ancylostoma ceylanicum*]
		GPLIN_000693600	105754-107423	bifunctional aminoacyl tRNA synthetase	no	GROS_g02020	porphyrin and chlorophyll metabolism
		GPLIN_000693700	107723-110938	u3 small nucleolar rna associated protein 14	no	GROS_g02019	ribosome biogenesis in eukaryotes
		GPLIN_000693800	111764-113032	succinate dehydrogenase cytochrome b560 subunit	no	GROS_g02018	defense response to Gram-negative bacterium
		GPLIN_000693900	113418-114209	'cold shock' DNA binding domain containing protein	no	GROS_g02017	sequence-specific DNA binding
283	SNP_283_56739	GPLIN_000814000*	56408-57804	BTB:POZ domain containing protein At1g55760	no		
		GPLIN_000814100	58370-60428	BTB:POZ domain containing protein At1g55760	no		
		GPLIN_000814200	61441-67930	transcribed hypothetical protein	yes	GROS_g13559	signal peptide
		GPLIN_000814300	68894-70678	BTB:POZ domain containing protein At1g55760	no		
		GPLIN_000814400	72618-73953	transcribed hypothetical protein	no		
		GPLIN_000814500	75558-76793	BTB:POZ domain containing protein At1g55760	no		
	SNP_283_56740	GPLIN_000814600	78642-79828	transcribed hypothetical protein	yes	GROS_g05788	signal peptide
		GPLIN_000814700	84623-91635	zinc metallopeptidase	no	GROS_g05789	metalloendopeptidase activity; peptidase family M13
		GPLIN_000814800	95043-97768	myelin transcription factor 1 protein	no	GROS_g14295	zinc finger, C2HC type
		GPLIN_000814900	107592-114130	transcribed hypothetical protein	no	GROS_g14213	BTB/POZ domain
		GPLIN_000815000	115751-116921	G patch domain containing protein	no		
296	SNP_296_8846	GPLIN_000832100**	6442-11746	Na:H eXchanger family member (nhx 9)	no	GROS_g04641 / GROS_g13418	protein F32B5.6, isoform j [*Caenorhabditis elegans*] / sodium:hydrogen antiporter activity
		GPLIN_000832200	12647-13096	transcribed hypothetical protein	no		
		GPLIN_000832300	17388-19554	transcribed hypothetical protein	no		

		GPLIN_000832400	33723-34555	transcribed hypothetical protein	no		
		GPLIN_000832500	35455-36989	transcribed hypothetical protein; Gpa_Dog_0189	yes		
		GPLIN_000832600	44182-46613	transcribed hypothetical protein	yes	GROS_g08307	lysosomal membrane
		GPLIN_000832700	47366-49673	lysosome associated membrane glycoprotein	yes	GROS_g08307	lysosomal membrane
		GPLIN_000832800	50657-51448	transcribed hypothetical protein	no	GROS_g08308	aminoacyl-tRNAhydrolase.
		GPLIN_000832900	52058-53243	14-3-3 protein	no	GROS_g05963 / GROS_g08309	neurotrophin signaling pathway / neurotrophin signaling pathway
		GPLIN_000833000	54914-56106	14-3-3 protein	no	GROS_g05963 / GROS_g08309	neurotrophin signaling pathway / neurotrophin signaling pathway
		GPLIN_000833100	63249-68201	calcium binding EGF domain containing protein	no	GROS_g08310	hypothetical protein Y032_0091g2492 [*Ancylostoma ceylanicum*]
338	SNP_338_98803	GPLIN_000903300	71992-78704	transcribed hypothetical protein	no		
		GPLIN_000903400	86045-87892	transcribed hypothetical protein	no	GROS_g03490	response to chitin
		GPLIN_000903500	89309-92938	serpentine receptor, class T family member	no	GROS_g06645	transmembrane
		GPLIN_000903600**	97414-99406	dorsal gland cell specific expression protein	no	GROS_g14146 / GROS_g14224	dorsal gland cell-specific expression protein [*Heterodera avenae*] / transmembrane; dorsal gland cell-specific expression protein [*H. avenae*]
		GPLIN_000903700	102236-103533	protein MICAL 3	no	GROS_g08157	LIM domain
		GPLIN_000903800	104125-104725	LIM domain containing protein	no		
		GPLIN_000903900	105988-106776	transcribed hypothetical protein	no		
		GPLIN_000904000	107274-107909	protein MICAL 3	no		
		GPLIN_000904100	108895-109595	transcribed hypothetical protein	no		
340	SNP_340_56189	GPLIN_000904700	24813-25894	transcribed hypothetical protein	no	GROS_g08025	SSF52540
		GPLIN_000904800	35241-37595	nematode astacin protease family member	no	GROS_g07035	extracellular region; metalloendopeptidase activity; Astacin-like metalloendopeptidase [*Strongyloides ratti*]

		GPLIN_000904900	37694-40604	peptidase M12A, astacin	no	GROS_g12919	astacin (peptidase family M12A)
		GPLIN_000905000	42995-45732	cell death protein 3	no	GROS_g12555	execution phase of apoptosis
		GPLIN_000905100**	53759-57940	transcribed hypothetical protein	no		
		GPLIN_000905200	75502-76417	transcribed hypothetical protein	no		
349	SNP_349_8349	GPLIN_000914300	13395-18410	zinc finger protein 280D	no	GROS_g11336 / GROS_g02450 / GROS_g11223	zinc finger protein [*L. loa*] / signal peptide / zinc finger C2H2 type domain signature
		GPLIN_000914400	31215-32425	transcribed hypothetical protein	no		
		GPLIN_000914500	63737-66258	transcribed hypothetical protein	no	GROS_g10058	signal peptide
		GPLIN_000914600	69418-70547	ubiquitin carboxyl terminal hydrolase 48	no	GROS_g03356	ubiquitinylhydrolase1
474	SNP_474_28528	GPLIN_001056200	3568-10018	transcribed hypothetical protein	no	GROS_g11538	zinc finger C2H2 type domain signature.
		GPLIN_001056300	10515-10989	transcribed hypothetical protein	no	GROS_g11539	transmembrane
		GPLIN_001056400	11106-12182	transcribed hypothetical protein	yes	GROS_g11539	transmembrane
		GPLIN_001056500	13710-14450	transcribed hypothetical protein	no		
		GPLIN_001056600	14570-20232	transcribed hypothetical protein	no	GROS_g11540	signal peptide
		GPLIN_001056700	52073-52540	transcribed hypothetical protein; Gpa_Dog_0074	yes		
		GPLIN_001056800	56482-58809	transcribed hypothetical protein	no		
		GPLIN_001056900	58931-60252	transcribed hypothetical protein	yes		
		GPLIN_001057000	62667-67109	transcribed hypothetical protein	no		
504	SNP_504_47039	GPLIN_001082800	211-620	protein containing SPRY domain	no	GROS_g14163	RBP-4 protein [*G. pallida*]
		GPLIN_001082900	11855-12808	paralog of RBP-5 protein (33H17)	no	GROS_g14179	RBP-1 [*G. pallida*]; signal peptide
		GPLIN_001083000	14667-16919	transcribed hypothetical protein	yes	GROS_g13008	hypothetical protein TcasGA2_TC001495 [*Tribolium castaneum*]

		GPLIN_001083100	18255-23950	transcribed hypothetical protein	yes	GROS_g10456	thap domain-containing protein 4 [*A. suum*]; transmembrane
		GPLIN_001083200	25548-26905	transcribed hypothetical protein	no		
		GPLIN_001083300	32640-39130	serine:threonine protein kinase SIK3	no	GROS_g10454	serine threonine-protein kinase kin-29 [*A. suum*]
		GPLIN_001083400*	43996-50149	3 hydroxy 3 methylglutaryl coenzyme A reductase	no	GROS_g10452	hmg CoA reductase A [*Polysphondylium pallidum* PN500]; protein homodimerization activity
		GPLIN_001083500	54107-59069	transcribed hypothetical protein	no	GROS_g10451	peptidase M10A M12B domain containing protein [*H. contortus*]; transmembrane; matrixin
782	SNP_782_20136	GPLIN_001257900	8259-9831	transcribed hypothetical protein	no	GROS_g14146	dorsal gland cell-specific expression protein [*H. avenae*]; putative esophageal gland cell protein Hgg-20 [*H. glycines*]
		GPLIN_001258000	16237-17191	transcribed hypothetical protein	no	GROS_g14213	BTB/POZ domain
		GPLIN_001258100**	19137-20558	paralog of RBP-1 protein; Gpa_Dog_0077	yes	GROS_g14234	RBP-1 protein [*G. pallida*]; secreted SPRY domain-containing protein 16, partial [*G. rostochiensis*]
		GPLIN_001258200	25107-27756	ubiquitin 40S ribosomal protein S27a 1	no	GROS_g07568	protein ubiquitination
		GPLIN_001258300	31187-31435	transcribed hypothetical protein	no		
		GPLIN_001258400	33199-34624	protein containing SPRY domain	no	GROS_g14184	RBP-4 protein [*G. pallida*]; secreted SPRY domain-containing protein 9 [*G. rostochiensis*]
988	SNP_988_7923 SNP_988_8037 SNP_988_8045 SNP_988_8100	GPLIN_001323400	2535-3808	transcribed hypothetical protein	no	GROS_g01568	protein of unknown function, DUF273
		GPLIN_001323500	12021-16917	serine:threonine protein kinase Nek6	no	GROS_g01334	serine/threonine-protein kinase Nek6, partial [*Bos mutus*]; cytokinesis; signal transducer activity
		GPLIN_001323600	19109-26588	Motor AXon guidance family member (max 2)	no	GROS_g10077	protein BM-MAX-2, isoform i [*B. malayi*]; K04409 Axon guidance
1243	SNP_1243_9865	no predicted gene					
1777	SNP_1777_961	GPLIN_001438500**	864-1181	transcribed hypothetical protein	no		
		GPLIN_001438600	2326-4922	maternal protein pumilio	no	GROS_g14286	cytosol
		GPLIN_0014	6616-7313	transcriptional regulator ATRX	no		

		38700					
3221	SNP_3221_1475	GPLIN_001518200	1511-2451	dorsal gland cell specific expression protein	no	GROS_g14143 / GROS_g14139	transmembrane; dorsal gland cell-specific expression protein [*H. avenae*] / transmembrane; dorsal gland cell-specific expression protein [*H. avenae*]
3816	SNP_3816_941				no predicted gene		
5159	SNP_5159_970				no predicted gene		

811